Study on the Instability Analysis of the Liquid Metal and Application for the Fusion Energy Conversion System

Fumito Okino

Contents

Chapter 0 Introduction

Chapter 1 Background information of this thesis
- 1.1 ITER TBM project
- 1.2 Tritium management in blanket
- 1.3 Previous studies on the tritium recovery from liquid PbLi
- 1.4 Motivation of this study

Chapter 2 Instability of the liquid metal column and droplet formation
- 2.1 Introduction
- 2.2 Theory
- 2.3 Experimental
- 2.4 Results and discussions
- 2.5 Conclusion

Chapter 3 Hydrogen isotopes mass transport on a falling liquid metal droplet
- 3.1 Introduction
- 3.2 Theory
- 3.3 Experimental
- 3.4 Results and discussions
- 3.5 Conclusion

Chapter 4 Tritium recovery device design for ITER scale fusion reactor
- 4.1 Introduction
- 4.2 Theory of the tritium extraction ratio
- 4.3 Design theory for the VST
- 4.4 Results and discussions
- 4.5 Conclusion

Chapter 5 Application of the instability theory for liquid first-wall feasibility
- 5.1 Introduction
- 5.2 Theoretical analysis
- 5.3 Experimental
- 5.4 Results and discussions

Chapter 6 Closing

6.1 Wrap-up conclusion of the thesis
6.2 List of presentations and publications
6.3 Acknowledgement

Ch. 0. Introduction

In this thesis, design of the tritium (^{3}H) extraction device with liquid metal PbLi droplets for fusion fuel supply, was studied by theory and by experimental. Instability theory and mass transport theory are main tools applied for the analysis. In addition, feasibility of a liquid metal film for fusion core first wall was analyzed as an application of the instability theory for another fusion engineering.

As an ongoing international fusion reactor experimental program, ITER (International Thermonuclear Experimental Reactor) is under construction now for aiming the first plasma at 2019 and DT burn at 2027. Within many ITER experimental programs, Test Blanket Module (TBM) Program is one of key elements for the future of fusion reactor. TBM program verifies the blanket system functions which perform the breeding and extraction of tritium as a fusion fuel, along with heat extraction and shielding function. Six parties of ITER members are proposing to fabricate their originated blanket system plan.

For the tritium extraction, two basic methods are so far short-listed. One is using the solid breeding material and the other is using the liquid breeding material. The solid breeder is generally regarded as a less challenging way than the liquid breeder. So, four of the above mentioned six TBMs are proposing to use solid breeding material.

However, the tritium extraction process using the solid breeder requires sophisticated chemical processes and energy consuming. Because the extracted output is consisted of Q_2(gas) and Q_2O(water), where Q means either of ^{1}H, ^{2}H, ^{3}H . On the other hand, the output from the liquid breeder is only gas as (HT or T_2), and has the possibility to perform simple and less energy consuming extraction. But by several reasons, it is regarded more challenging way, right now.

This study aimed to re-evaluate the liquid PbLi tritium extraction as a viable and less energy promising method. By series of theoretical analysis and experimental verifications, the tritium extraction from droplet of liquid PbLi showed prominent high efficiency than other methods. The oscillating deformation of a droplet contributed the high efficiency. Then, by using the attained results, case study design of the tritium extraction device for the ITER class reactor is performed. The attained device size showed as acceptable for production.

Through this study, the instability theory showed as a strong analysis tool, and applicable for various liquid film engineering. So, as an application, the feasibility of the liquid film first wall for high energy flux protection was studied.

In Section 1, background information of the tritium extraction methods are explained. Configurations of ITER-TBM, brief explanation of the differences of solid and liquid breeding methods, previous studies, are described. Then the motivation and purpose of this study are explained.

In Section 2, droplet formation from the liquid metal PbLi is studied. The relation between the droplet diameter and the nozzle diameter is a key function for the extraction device design.

By using the instability theory, i.e. Plateau-Rayleigh instability, the equation to describe the droplet diameter from a nozzle is theoretically deduced. The deduced equation suggests the droplet diameter is merely depends on the nozzle diameter, and no relation with other physical properties of the liquid media, as far as in the surface tension dominating regime. By the experimental, which uses four different diameter nozzles from 0.4 mm to 1.0 mm, the droplet diameter is measured with water and liquid metal PbLi case. The results well accorded with the theory. Also by the high speed movie camera, the oscillating deformation on the sphere is observed. By this result the droplet oscillation model is constituted.

In Section 3, this is the main event of this thesis, the mass transfer rate of hydrogen isotopes on the liquid PbLi droplet while falling in vacuum, is studied. It is a critical figure which must be determined to design the tritium extraction device.

The mass transfer rate by previous reports deviated more than magnitudes of orders, and it was regarded due to the ambiguous solubility effects of each experiment. The conservative safety estimation of the extraction device must use the lower transfer rate, then resultant device size is enormously huge and it has been regarded as un-realistic method. This is one of decisive reasons that many TBM models did not choose the liquid breeding material.

The author deduced the ingenious experimental method to eliminate the ambiguous solubility effects and identified the mass transfer rate of hydrogen isotopes on a falling droplet. The keystone is to divide the released amounts of different diameter droplets by each other, and eliminate the solubility effects. The result showed two orders of magnitudes higher mass transfer rate than that of the static condition. This result accorded with pre-performed theoretical estimation based on the droplet oscillation model, which is observed in previous experimental. Falling droplet in vacuum is under dynamic condition, so this result confirmed an another mass transfer mechanism must occur under this phenomenon.

In Section 4, the size of the tritium extraction device for ITER class fusion reactor is studied by engineering methods.

The attained results of mass transport from a falling droplet showed two orders of magnitudes higher value than that of the previous value under static condition. By this result, the design window of the tritium extraction device using the falling droplet is drastically enlarged. The device size is expected to be smaller and comparable with the other methods.

By a case study of ITER class fusion reactor, the inner diameter of the tritium extraction chamber is 2.5 m and the dropping height is 0.25 m. This size is comparable or smaller than the other methods. This case study is based on the high PbLi flow blanket model, and in case of low PbLi flow model like EU-HCLL, the corresponding device size is considered to be further smaller. The reasonable extraction ratio of tritium from the safety point of view also discussed.

In Section 5, a feasibility of liquid metal film for a fusion core first wall is studied as an application of the instability theory. The fluctuation of the film thickness of liquid first wall is the problem for the high energy flux protection of a blanket, divertor, and ICF core wall.

The two dimensional film flow instability is analyzed by using the K.H. instability theory, and the critical condition of the film fluctuation under ambient gas pressure is deduced. This result is supported by an experimental using a water instead of a liquid metal. This study suggests that the self-evaporating gas pressure of liquid film PbLi might be cause of the film thickness instability, even though inside of the fusion core is commonly regarded to be in pure vacuum.

In Section 6, wrap-up conclusions achieved from this study, and other miscellaneous matters are described.

Ch. 1. Background information of this thesis

Summary of this chapter

The solid breeder blanket and the liquid breeder blanket are to be tested in ITER-TBM Program. The solid breeder blanket is generally recognized as a less challenging method due to the pre-established techniques, even though it consumes much process energy. Liquid breeder method using droplet extractor is a simple less process energy consuming way, but generally regarded as un-realistic by negative results of previous studies. To re-evaluate the liquid breeder and establish a less process energy method is a motivation of this thesis.

1.1. ITER-TBM project

As a first stage, ITER-TBM Project (International Thermonuclear Experimental Reactor - Test Blanket Module Project) is a good guide-post to understand the background of this thesis. The report “Overview of the ITER TBM Program” by Giancarli et al. [1] clearly and simply depicted about this program, so I recapitulate this report. Hereafter the explanation surrounded with “ ” means the quoted phrases from the original report.

1.1.1 Objective of the ITER TBM

The objective of the ITER-TBM Program is described as “ provide the first experimental data on **the performance of the breeding blankets in the integrated fusion nuclear environment** ”.

Key function of the breeding blanket is described as “ **Can tritium be produced in the blanket and extracted from the blanket** at a rate equal to tritium consumption in the plasma plus losses by radioactive decay from tritium inventories in reactor components ? ”.

Another key functions of the breeding blanket are the heat extraction and shielding function from high energy fluxes, but they are out of the scope of this thesis.

1.1.2 Configuration of ITER-TBM

The configuration of the TBM is described as “ It foresees **to test six mock-ups of breeding blankets**, called Test Blanket Module (TBM) ..... from the beginning of the ITER operation.”

The above mentioned, six mock-ups are listed on a Table-1. Some key points for the breeding material are summarized below. As an example of the breeding blanket, an image of the HCLL TBM is shown at Fig. 1.[13]

a) Two different types of breeding material are proposed. Two parties are using liquid eutectic PbLi and four parties are using solid pebble Li_4SiO_4 or Li_2TiO_3.
b) EU team verifies two different TBM models.
c) Japanese team chose the WCCB, water cooling with solid breeding material method.

Table-1. The configuration of the six TBMs by L.M. Giancarli et al.[1], Cho et al. [14], P. Chaudhuri et al. [15], K.M. Feng et al. [16]

Nr.	Type	Breeding	Cooling	Member	Port
1	HCLL	Liquid; eutectic metal **PbLi**	Helium	EU	#16
2	HCPB	Solid; Li_4SiO_4 or Li_2TiO_3 pebble beds	Helium	EU	#16
3	WCCB	Solid; Li_2TiO_3	Water	Japan	#18
4	HCCR	Solid; Li_4SiO_4 or Li_2TiO_3	Helium	Korea	#18
5	HCCB	Solid; Li_4SiO_4	Helium	China	#02
6	LLCB	Solid+Liquid; Li_2TiO_3+ **PbLi**	Helium	India(Russia)	#02

Two different types of breeding material are proposed. One is using liquid eutectic PbLi and the other is using solid pebble Li_4SiO_4 or Li_2TiO_3.

The cooling media is also grouped into two groups, one is using helium gas and the other is using liquid media, water or liquid PbLi.

Abbreviations; PbLi (Eutectic metal Pb-17Li), HC (Helium Cooled), LL (Lithium Lead), PB (Pebble Bed), WC (Water Cooled), CB (Ceramic Bed), DC (Dual Coolant)

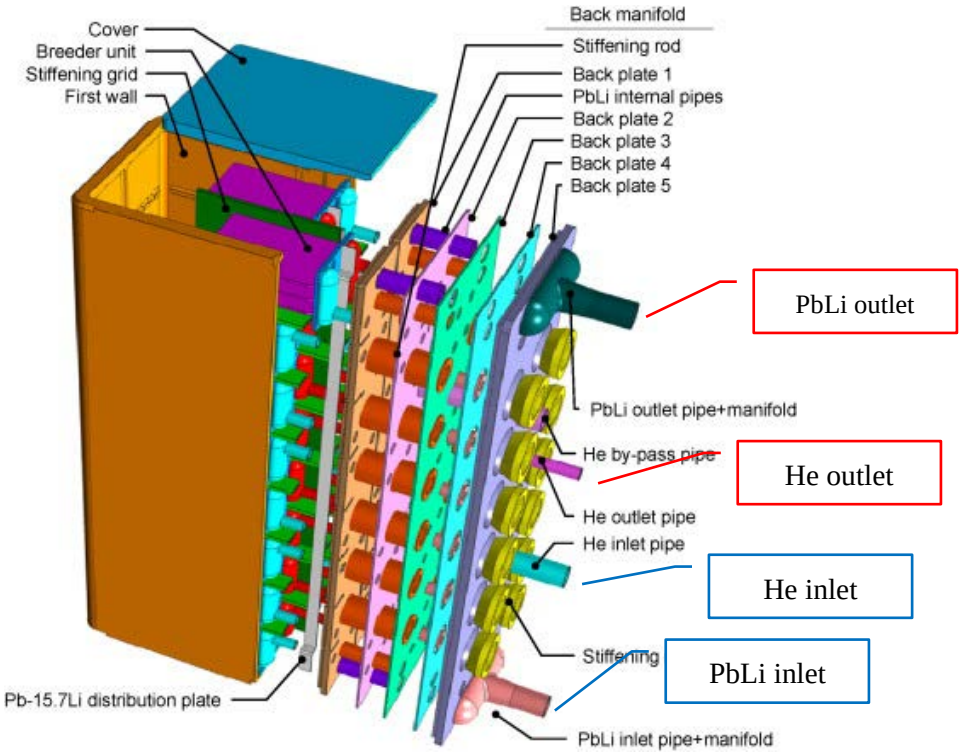

Fig. 1. An exploded view of the HCLL-TBM, by F. Gabriel et al. [13]

Helium Cooled Lithium Lead (HCLL) Test Blanket Module(TBM) proposed by EU is depicted. Helium gas is used as a cooling media, and liquid eutectic metal Pb-17Li is used as a breeding material.

1.1.3 Test Blanket System (TBS) design

The test blanket system is described as " TBMs are connected with several ancillary systems, such as cooling systems, **tritium extraction systems**, coolant purification systems, and instrumentation and control (I&C) systems. TBMs and associated systems are called Test Blanket Systems (TBSs)."

Fig. 2 shows the image of the TBS by V. Boccaccini et al. [2] It is consisted of TBM, Pipe forest and Ancillary Equipment Unit (AEU).

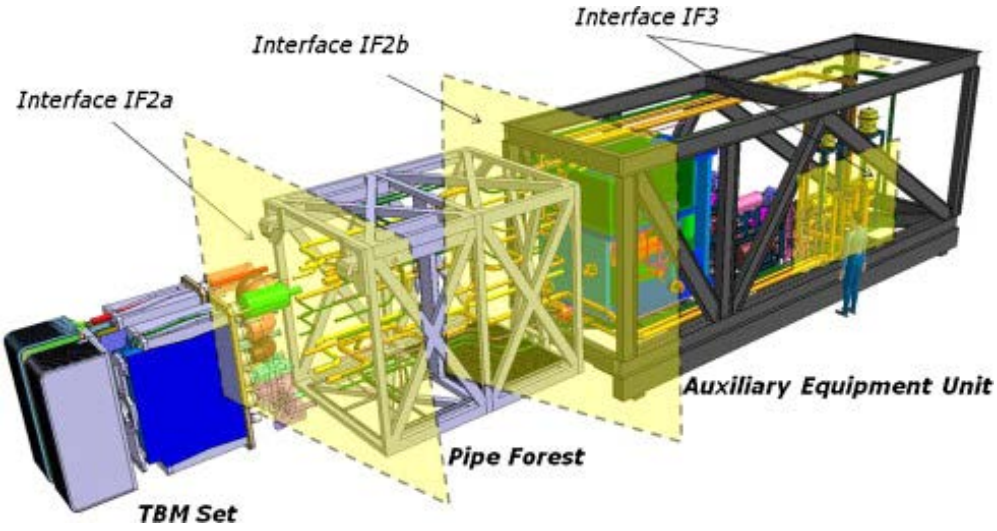

Fig. 2. An image of the TBS by V. Boccaccini et al. [2]

TBMs are connected with several ancillary systems, such as cooling systems, tritium extraction systems, coolant purification system, and instrumentation and contro(I&C) systems. TBMs and associated systems(pipe forest, auxiliary Equipment unit) are called Test Blanket Systems(TBSs).

1.1.4 TBM Program management

The program management is described as "... to perform the TBM Program in an **efficient and timely manner**." [2]

This term implies that TBM Program is a project to verify the total-system feasibility with pre-established methods proposed by each members, and not the place to examine the new un-established methods. The long term TBM testing plan by V.A. Chyanov et al. [3] is attached on Fig. 3. Due to the ITER working conditions, ex. the size scale of the device, international co-operation etc., to maintain this schedule in an efficient and timely manner, is considered a quite high hurdle project.

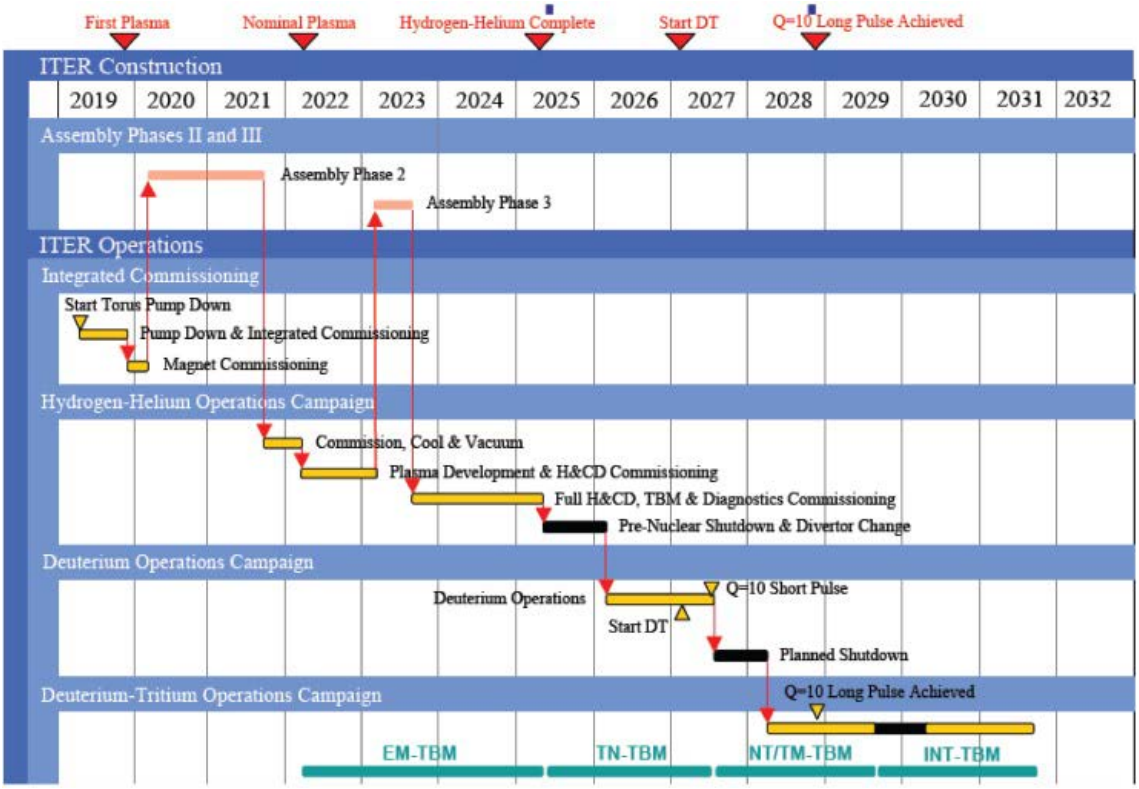

Fig. 3. TBM testing plan by Chuyanov et al. [3]

TBMs are scheduled to be installed at the first stage of operation. Testing plan is integrated with four campaigns as, Integrated Commissioning, Hydrogen-Helium Operation Campaign, Deuterium Operations Campaign, and Deuterium-Tritium Operations Campaign. Main official steps are the First Plasma End of 2019, and the Start DT End of 2026. It is required to perform in an efficient and timely manner. Note; The original time schedule is quoted.

1.2 Tritium management in blanket - open issues

The ITER-TBM Program is roughly overviewed in previous section. Within various ITER research programs, my attention is focused on the tritium breeding and tritium extraction method by using a liquid PbLi. It is a only on-going project about the fusion reactor and fusion fuel research. To understand the up-to-date situation about the tritium management and breeding blanket of ITER program, particularly for the tritium extraction issues, following paper

“ Tritium management and safety issues in ITER and DEMO breeding blankets” by B. Bornschein et al. [4] is introduced.

It describes at the abstract “ The present paper gives an overview of tritium management in breeder blankets. ....open tritium issues are discussed, thereby focusing on **tritium extraction from blanket**, coolant detritiation and tritium analytics and accountancy, necessary for accurate and reliable processing as well as for book-keeping.”.

1.2.1 Two classes of blankets “solid blankets and the liquid ones”

Two classes of the blankets are described as “Basically, two classes of blankets are existing; **the solid blankets and the liquid ones** .... each blanket concept requires a blanket specific **tritium extraction system** (TES) being an essential part of the outer fuel cycle.” The comparison table is copied below in Table-2.

Table-2. Selection of breeder blanket concepts by B. Bornshcein et al. [4]

	Solid	Liquid
Breeder material	Ceramic materials: LiO2, LiAlO2, Li2SiO3, Li4SiO4, Li8ZrO6, Li2TiO3	**Li17Pb83**, Flibe (LiF and BeF2)
Neutron multiplier	Be, Be12Ti	Pb, Be
Coolant	Helium cooled, Water cooled	Helium cooled, Water cooled, Self-cooled, Dual cooled
Advantages	**Tritium extraction less challenging**	**No breeder damage or swelling, Adjustable breeder composition**
Difficulties	Blanket replacement, tritium permeation into coolant	Magneto-hydro-dynamic, corrosion, tritium permeation into coolant
EU-TBM concept	Helium cooled pebble bed (HCPB)	Helium cooled lithium lead (HCLL)
Principal investigator	KIT	CEA, CIEMAT, ENEA

The pros and cons of the two breeding materials, solid and liquid, are summarized. The advantage of solid breeder is described as “Tritium extraction less challenging”.
The advantages of the liquid breeder is “ no-swelling, adjustable composition”.
As a common difficulties, “permeation into coolant” is listed.

1.2.2 Tritium extraction method

Key differences of the two methods of tritium extraction are described as follows, and a schematic is attached in Fig. 4..

(a) "...one needs to purge the breeder material with an inert gas to separate the tritium from the breeder material. This is done by **purging directly through the solid blanket** or,
(b) "...in case of liquid blanket, **through a gas liquid contactor** outside of the blanket."
(c) " ...the **liquid breeder** where **tritium is extracted in molecular form (HT, T_2)**"
(d) "...in **solid breeder** tritium will appear in **molecular(Q_2) and oxidized form (Q_2O) (water)**". Q is either of ^1H, ^2H, or ^3H.
(e) "...these processes are exclusively either for **Q_2 or Q_2O, a two-stage process is necessary** to fully recover the tritium from the blanket."

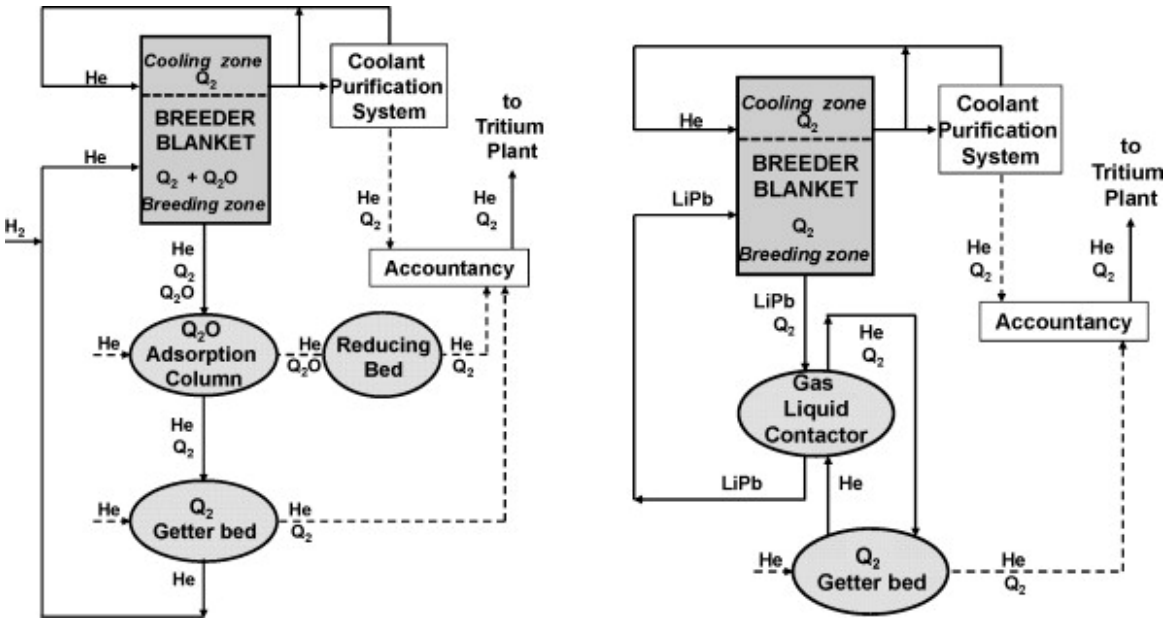

Fig. 4. A schematic of TES concepts for a solid breeder (left) and a liquid one (right) by B. Bornschein et al. [4].

In the solid case (left), a two-stage process is necessary to remove tritium in molecular Q_2 and oxidized form Q_2O (water), where Q means either of ^1H,^2H, or ^3H. H_2 is again added for He make-up.
On the other hand, in the liquid case (right), one stage process is enough, because tritium is extracted in molecular form (HT, T_2). The concept of tritium direct extract in vacuum, which is the main theme of this thesis,

is not mentioned here. The dashed lines indicate the regeneration processes for the getter bed and the molecular sieve."

1.2.3 Details of tritium extraction by solid breeding material

Then, to obtain further understanding of the tritium extraction process by solid breeding material, the report "Tritium recovery from an ITER ceramic test blanket module – process options and critical R&D issues" by H. Albrecht and E. Hutter.[5] is examined. This paper simply explains the process of solid breeder tritium extraction methods by FZK, though some portion is not up-to-date one. The extraction processes are described as follows, and the process flow sheet is shown at Fig. 5.

(a) HTO and H_2O are frozen out in a **cold trap** operated at ≤ **-100 ºC**; at ④ of Fig. 5.

(b) HT, H_2, and gaseous impurities are **adsorbed** on a molecular sieve bed operated at **-195 ºC**. at ⑥-a of Fig. 5.

(c) The clean helium is then sent through a make-up unit where **hydrogen is again added** to provide a He:H_2 swamping ratio of 1000; at ⑨ of Fig. 5.

(d) Desorption of the hydrogen isotopes from the molecular sieve bed is carried out in a secondary loop containing a circulation pump and a Pd/Ag diffuser; ⑥-b,⑭,⑮ of Fig. 5.

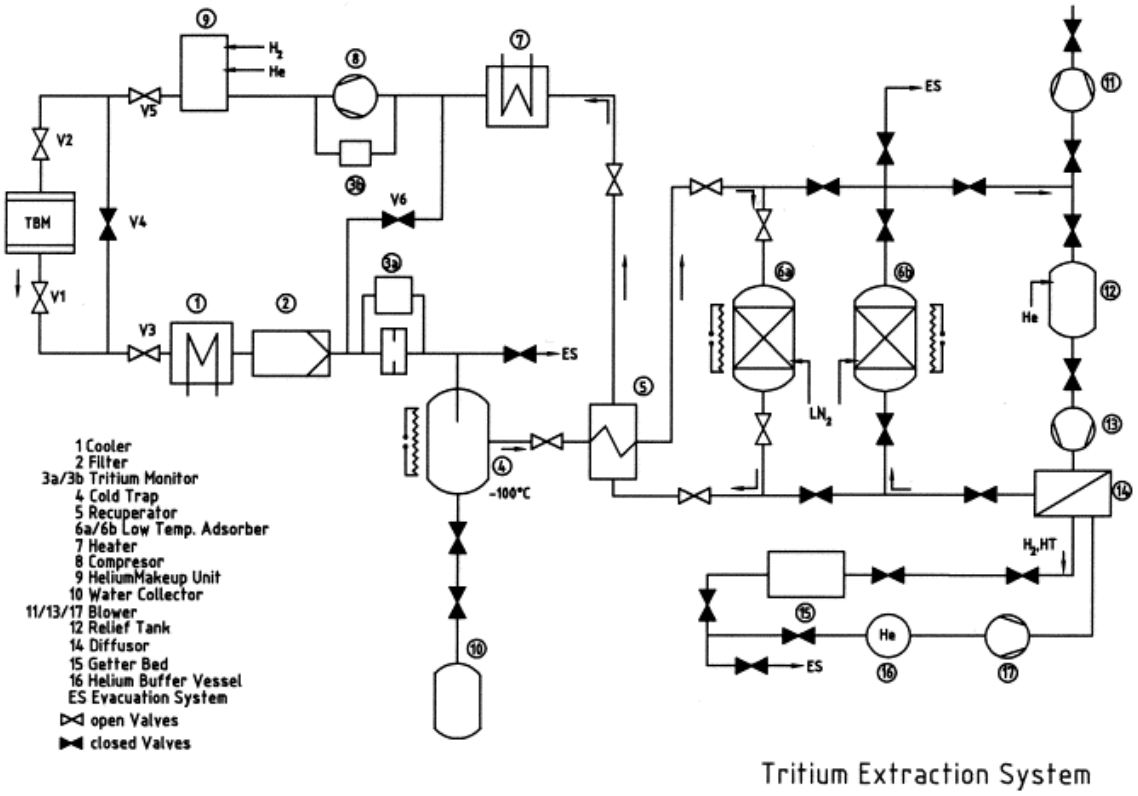

Fig. 5. Process flow sheet of the tritium extraction system by H. Albrecht et al. [5].

(a); HTO and H_2O are frozen out in a **cold trap** operated at ≤ -100ºC; at ④.

(b); HT, H_2, and gaseous impurities are **adsorbed** on a **molecular sieve bed** operated at -195 ºC. at ⑥-a.

(c); The clean helium is then sent through a make-up unit where **hydrogen is again added to provide a He:H_2 swamping** ratio of 1000; at ⑨.

(d); Desorption of the hydrogen isotopes from the molecular sieve bed is carried out in a secondary loop containing a circulation pump and a Pd/Ag diffuser; at ⑥-b,⑭,⑮.

①;Cooler ④;Cold Trap ⑥-a,-b; Low Temp. Adsorber ⑦;Heater

⑨; Helium make-up ⑩; Water Collector ⑭; Diffusor ⑮; Getter bed

As seen from Fig. 4, the tritium separation process by solid breeding material, is consisted of already established methods, written in the comparison table-2 as “tritium extraction less challenging”. However it is a much process-energy consuming method, due to the hydrogen swamping.

1.3 Previous studies on the tritium recovery from liquid PbLi

In this section, the tritium extraction method from liquid PbLi is surveyed through the report “Tritium recovery from liquid metals” by H. Moriyama et al.. [7] It describes about the liquid breeding material as

“ Liquid breeder materials have **many inherent advantages** over solid breeder materials, and the liquid metals pure lithium and **Pb-17Li** alloy are expected to be **potential candidate materials**. This paper reviews recent work on tritium recovery from the two candidate materials, and discusses the implications of the **work for successful future development**...”.

This sentence has masterminded the evaluation of the liquid PbLi blanket media until now. Even the latest report about the tritium management [4] still quotes this sentences. To understand the controversies between the “many advantages” and the “future development”, above paper is carefully examined.

1.3.1 Assessment report by H. Moriyama et al.

The tritium recovery from liquid PbLi, H. Moriyama et al.[7] focused on the liquid-gas contactor method, particularly the bubble column and the droplet spray method. As the downside of the methods, they discussed the unreliable tritium desorption rate and the estimated device size.

As the unreliable tritium desorption rate, it described “ For evaluating the tritium recovery method from Pb-17Li with gas or vacuum, a knowledge of **tritium desorption rate constant** is required. ...but **they are very scattered** since the surface nature is influenced by many factors.” Fig. 6 is the plots of tritium absorption and desorption rate shown by Moriyam et al..

The two data which showed high mass transfer coefficient by Terai and by Viola on Fig. 6 are proved to have theoretical reasoning, in this thesis. But it was regarded as the influence by surface nature.

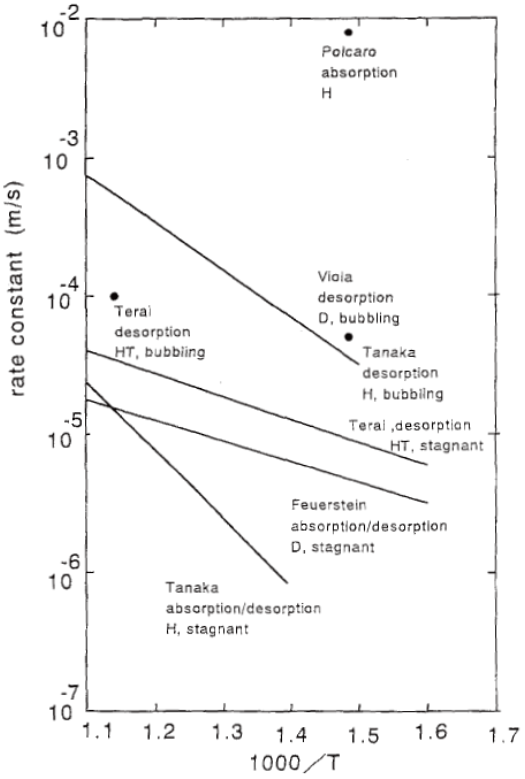

Tritium absorption and desorption rate constants (or mass transfer coefficient) for liquid Pb–17Li.

Fig. 6. Tritium absorption and desorption constants (mass transfer coefficient) for liquid Pb-17Li , by Moriyama et al. [7]

The vertical axis is the mass transfer coefficient [m/s] and the horizontal line is the reciprocal of the temperature [1000/K].

The previously reported data of the mass transfer constants of tritium from liquid PbLi deviated approximately two orders of magnitudes. Moriyama et al. described “For evaluating the tritium recovery method from Pb-17Li with gas or vacuum, a knowledge of **tritium desorption rate constant** is required. ...but **they are very scattered** since the surface nature is influenced by many factors.”

The two data which showed high mass transfer coefficient by Terai and by Viola are proved to have theoretical reasoning, in this paper. But it was just regarded as the influence by surface nature.

1.3.2 The study by G. Pierini

The device size matter, another downside issue of liquid breeding method, was based on the previous study by G. Pierini [6], then it is surveyed hereafter.

1.3.2.1 Analytical model

Pierini analytically examined the relation between the tritium extraction ratio and the corresponding device size by two methods, the bubble extractor and the droplet spray extractor, as shown in Fig. 7-1 and Fig. 7-2, respectively.

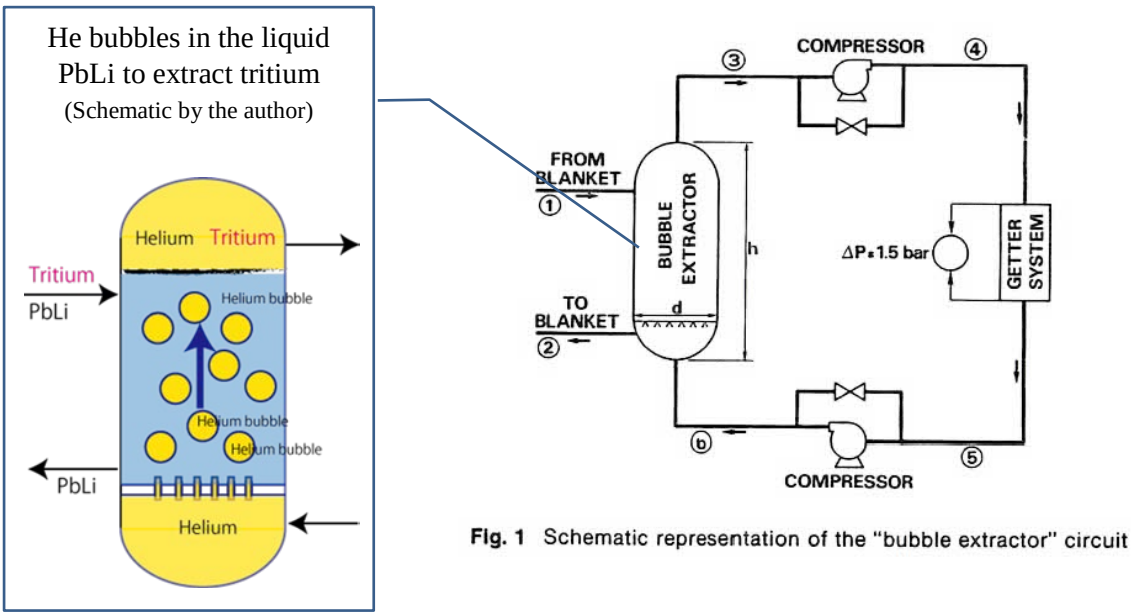

Fig. 1 Schematic representation of the "bubble extractor" circuit

Fig. 7-1. Schematic representation of the "bubble extractor" circuit by G. Pierini [6]**.**

Additional schematic (left) added by the author.

The liquid Pb-17Li is continuously pumped out from the blanket and passed from the top ① to the bottom ② of the extractor. The helium is pumped to the bottom of the extractor ⑥ against the flow of the eutectic and ③→④→⑤ recycled through the getter units where the tritium is quantitatively removed from the helium stream.

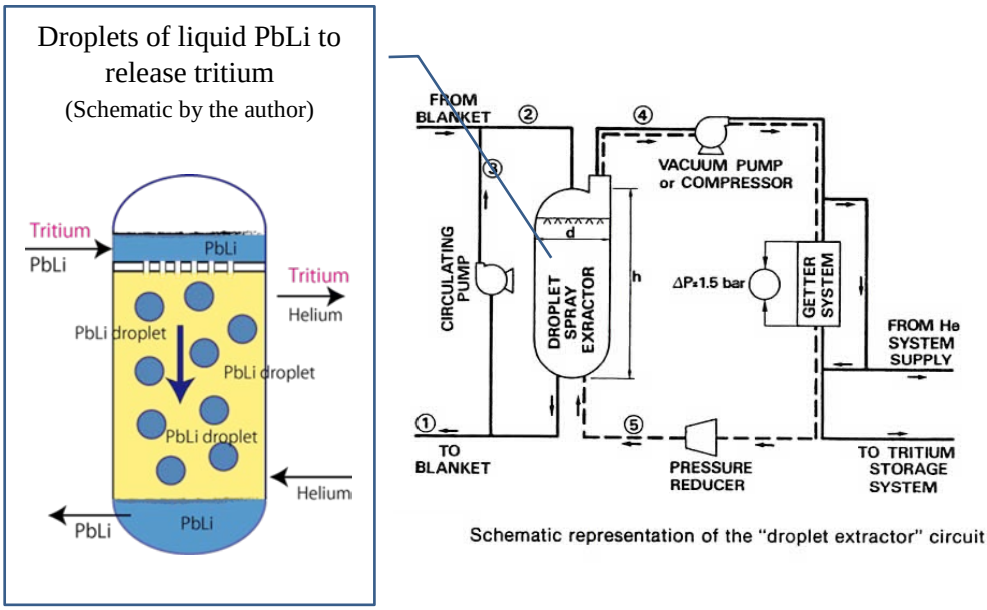

Fig. 7-2. Schematic representation of the "droplet spray extractor" circuit by G. Pierini [6]**.**

Additional schematic (left) by the author.

The liquid Pb-17Li is continuously pumped out from the blanket and passed from the top ② to the bottom ① of the extractor as the rain of small droplets produced by a series of spray nozzles. The tritium can be recovered from the rain of small droplets in two ways: by direct vacuum pumping, and by circulating a helium stream countercurrent to the liquid droplets.

1.3.2.2 Operation principal and case study results

Pierini assumed following hypothesis as an operation principal, and performed case studies. Mathematical details are listed at Appendix-A, end of this chapter.

(a) The tritium mass transport mechanism is same for both from liquid PbLi flow to helium bubble, and from droplet PbLi to helium sweep gas or in vacuum condition.

(b) The rate of mass transport at the boundary surface between the liquid and the gas phase, is balanced with the rate of surface recombination. The rate of surface recombination is rather lower value, and it governs the rate of mass transport. Pierini evaded the scattering mass transfer rate problem by this hypothesis.

(c) The rising velocity of a bubble in liquid PbLi is determined by the terminal velocity of a bubble in liquid. The falling velocity of the droplet is determined by the gravitational acceleration.

The case study results of the bubble extractor and the droplet spray extractor are shown at Fig. 8 and Fig. 9, respectively. The height of bubble extractor in Fig. 8, is approximately plotted between 10 cm and 100cm (1 m), and the diameter of the device is between 300 cm and 100 cm. On the other hand, in case of the droplet spray extractor in Fig. 9, the height of extractor is approximately plotted between 10 cm and 4000 cm (40 m). The diameter of the extractor also plotted between 20 cm and 4000 cm. The result showed that in case of the droplet spray extractor, the device size is approximately 10 times larger than the device size of the bubble extractor.

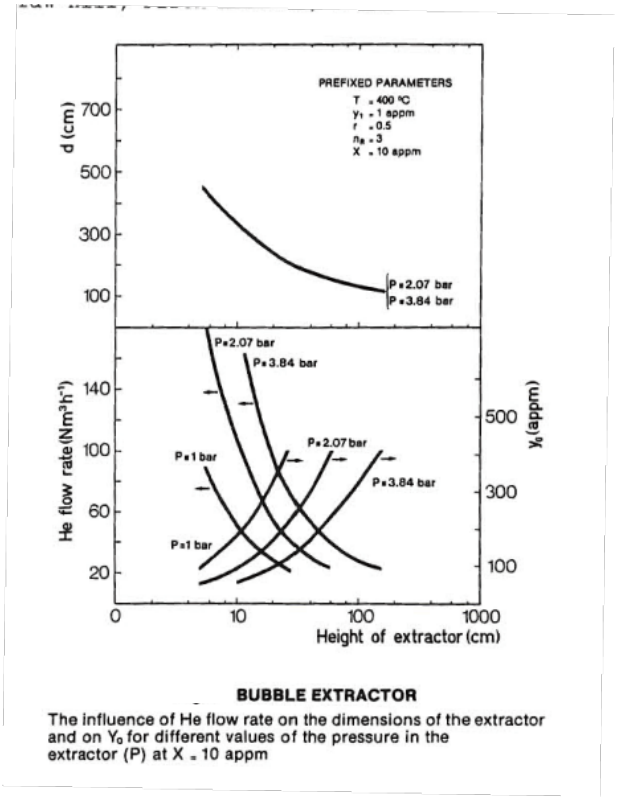

Fig. 8. Case study results of the bubble extractor, by G. Pierini [6]

The horizontal axis is the height of bubble extractor in cm. The vertical axis is the device diameter in cm and helium gas flow rate as a function of various gas pressure.

The height of bubble extractor is approximately plotted between 10 cm and 100 cm. The diameter of the device is between 100 cm and 300 cm.

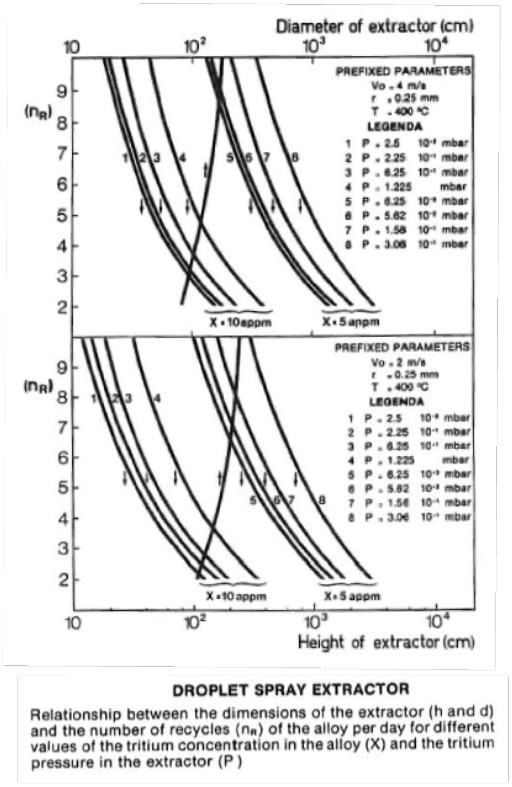

DROPLET SPRAY EXTRACTOR

Relationship between the dimensions of the extractor (h and d) and the number of recycles (n_R) of the alloy per day for different values of the tritium concentration in the alloy (X) and the tritium pressure in the extractor (P)

Fig. 9. Case study results of the droplet spray extractor, by G. Pierini [6]

The horizontal axis is the height of extractor in cm. The vertical axis is the number of liquid recycles per day as a function of various tritium concentration.

The height of extractor is plotted between 10 cm and 4,000 cm (40 m). The diameter of the extractor also plotted between 20 cm and 4,000 cm.

Pierini concluded that "**It seems more appropriate to use the bubble extractor rather than the droplet spray one**.

1.3.2.3 Pierini's conclusion

By comparing the calculated results shown in Fig. 8 and Fig. 9, particularly by the difference of the device size, Pierini concluded as "**It seems more appropriate to use the bubble extractor rather than the droplet spray** one because this last requires the development

of particular systems for distributing the liquid alloy in very small droplets". The advantage of the droplet in vacuum is not distinguished from the droplet in helium.

1.3.3 Discrepancies to the previous studies on the tritium extraction from liquid PbLi

By carefully examine the previous studies, the author obtained following discrepancies to the theoretical analysis of these tritium extraction methods.

1.3.3.1 The scattering of the tritium absorption and desorption constants

In Fig. 6, the scattering of the tritium absorption and desorption constants by previous studies are considered as the mere scattering by the different surface nature of each experiment. However, the plots show the difference of the attained results by bubbling and in stagnant condition. Three data attained by bubbling showed almost same high order of mass transfer coefficients. The author considered that some another mechanism exists on this methods different with the stagnant condition, and the orders of scattering might be not only by the surface nature difference.

1.3.3.2 The mass transfer coefficient

Pierini used the mass transfer coefficient of tritium at the boundary of liquid and gas phase described as equation (3) which was quoted from the previous study by T.K. Sherwood [8]. However, this equation was deduced for the flow field **in laminar creeping flow around a sphere**. So this equation might be applicable for the "bubble extractor" of which the helium bubble flows through liquid PbLi. But it is worth re-consideration to apply this equation for the "falling droplet spray" condition, particularly in case of in vacuum, no continuous flow around a sphere exists.

1.3.3.3 Mass flux in liquid phase and surface recombination flux

Pierini assumed that the amount of mass flux at liquid boundary phase is balanced with that of the recombination rate on the interface surface as shown below

$$\rho_l k_l \left(x_b - x \right) = K_d x^2 - K_a P_{T_2} \quad (1),$$

where the L.H.S. of the above equation describes the mass transfer flux at the boundary of liquid and gas phase, the R.H.S. describes the tritium desorption and sorption flux on the surface

of a droplet. Coefficients K_d and K_a means the desorption rate and sorption rate constants, respectively.

However, these coefficients K_d and K_a were attained on the **experiment under equilibrium condition**.[9] The interface of the gas bubble rising in PbLi or falling droplet, particularly in vacuum, is considered **under dynamic condition**. It is worth re-examination whether these coefficients are also applicable for the dynamic condition.

1.4 Motivation of this study

The generally recognized conclusion of tritium extraction method is that the solid breeder is **less challenging way**. So, it is reasonable that many ITER parties chose the solid breeding methods.

However, the tritium extraction from solid breeder requires many chemical processes and much process energy as described in Sec. 1.2. This might undermine the energy balance of the fusion system in near future. On the other hand, the liquid breeder has a possibility of less energy consuming method. Particularly the **tritium direct extraction in vacuum,** which is not using the helium purge gas, is the least energy consuming method even though it is not recognized as a viable method right now.

By this reasoning and some discrepancies to the previous studies, the author decided to work on “the tritium direct extraction in vacuum” as a main subject of the thesis and performed series of studies to establish a viable method of it. It is considered to realize what Moriyama et al. described in 1995 as “ Liquid breeder materials have **many inherent advantages** over solid breeder materials, and the liquid metals **Pb-17Li** alloy are expected to be **potential candidate materials**.....the implications of the **work for successful future development**...”.[7]

Almost 40 years ago, T.K. Sherwood already suggested the possibility of high efficiency extraction from a droplet in his literature “Mass Transfer” published in 1975, unfortunately it is out of print now [8]. It is not exactly mentioned about the extraction in vacuum, but it encouraged me to challenge the subject.

Appendix A

The study by G. Pierini

The mathematical details of the study by G. Pierini [6] is described here.

A.1 Models

Two methods, the bubble extractor and the droplet spray extractor were analytically examined, as shown in Fig. 7-1 and Fig. 7-2 in Ch.1, respectively.

A.2 Operation principal of the bubble extractor (Fig. 7-1)

The rise velocity of the bubble is approximated by the terminal rise velocity which is given by the expression

$$v = \left[\frac{8rg}{3c_t} \right]^{1/2} \quad (1),$$

where Ct assumes the value of 0.8."

"The tritium flow rate in the liquid phase can be given by the relation

$$J = \rho_l k_l \left(x_b - x \right) \quad (2)$$

where ρ_l is the density of liquid, x , x_b is the tritium concentration in liquid eutectic, b is at bulk, and k_l is the mass transfer coefficient in liquid phase which is described by Sherwood Ch.1-[8] as

$$k_l = \left[\frac{D^2 v}{4r^2} \right]^{1/3} \quad (3)$$

"The $2T \rightarrow T_2$ recombination rate at the interface according to Ch.1-[6] is given by the relation

$$J = K_d x^2 - K_a P_{T_2} \quad (4)$$

where K_d , K_a is Specific tritium desorption rate and Specific tritium absorption rate, respectively.

By combining above two flux equations(2),(4) as equivalent, and merging (1) and (3), Pierini deduced the equation of the tritium concentration in gaseous phase at the bubble extractor as

$$Y_0 = Y_1 F + cK_d x^2 \int_{\sqrt{P_0}}^{\sqrt{P_1}} F \, \mathrm{d}\sqrt{P} \tag{5}$$

where F , c is independent additional expression which is eliminated here.

A.3 Operation principal of the droplet extractor (Fig. 7-2)

In the extractor, the falling speed of the droplet is given by

$$v = \left[{v_0}^2 + 2gh \right]^{1/2} \tag{6}$$

Analogous consideration to those made for the bubble extractor are valid in this case. Then the tritium enrichment in the liquid stream is given by

$$-L dx = ds\left(K_d x^2 - K_a y P \right) \tag{7}$$

where L , y, P is the liquid eutectic flow rate, the tritium concentration in gaseous phase, and the pressure , respectively. Then finally, the tritium concentration in liquid eutectic is deduced as

$$\mathrm{Ln}\left[\left(\frac{x - x_{eq}}{x_0 - x_{eq}} \right) \left(\frac{x_0 - x_{eq}}{x_1 + x_{eq}} \right) \right] = -x_{eq} \frac{3K_d}{2\rho_l r g} \left[\sqrt{2gh + {v_0}^2} - v_0 \right] \tag{8}$$

where x_{eq} is the concentration at equilibrium condition.

References

[1] L.M. Giancarli, M. Abdou, D.J. Campbell, V.A. Chuyanov, M.Y. Ahn, M. Enoeda, C. Pan, Y. Poitevin, E. Rajendara Kumar, I. Ricapito, Y. Strebkov, S. Suzuki, P.C. Wong, and M. Zmitko, Overview of the ITER TBM Program, Fusion Engineering and Design **87** (2012) 395-402.

[2] L.V. Boccaccini, A. Aiello, O. Bede, F. Cismondi, L. Kosek, T. Ilkei, J.-F. Salavy, P. Sardain, L. Sedano, and European TBM Consortium of Associates, Present status of the conceptual design of the EU test blanket systems, Fusion engineering and Design **86** (2011) 478-483.

[3] V.A. Chuyanov, D.J. Campbell, and L.M. Giancarli, TBM Program implementation in ITER, Fusion Engineering and Design **85** (2010) 2005-2011.

[4] B. Bornschein, C. Day, D. Demange, and T. Pinna, Tritium management and safety issues in ITER and DEMO breeding blankets, Fusion Engineering and Design **88** (2013) 466-471.

[5] H. Albrecht and E. Hutter, tritium recovery from an ITER ceramic test blanket module – process options and critical R&D issues, Fusion Engineering and Design **49-50** (2000) 769-773.

[6] G. Pierini, Feasibility Study of Tritium recovery Systems from 83PB17LI Breeding Material of a D-T Fusion Reactor, Fusion technol. (1984) Vol. 1 pp463-471.

[7] H. Moriyama, S. Tanaka, D.K. Sze, J. Reimann, and A. Terlain, Tritium recovery from liquid metals, Fusion engineering and Design **28** (1995) 226-239.

[8] T.K. Sherwood, R.L. Pigford, and C. R. Wilke, Mass Transfer, 1975, McGraw-Hill, Inc., ISBN 0-07-056692-5.

[9] G. Pierini, A.M. Polcaro, P.F. Ricci, and A. Viola, Perspectives for tritium recovery from liquid Pb83Li17 alloy, Commission of the European Communities, EUR 8599 EN (1983).

[10] F. Charru, Hydrodynamic Instabilities, translated by P. De Forcrand-Millard, Cambridge University Press (2011), ISBN 978-0-521-76926-6

[11] R. B. Bird, W. E. Stewart and E. N. Lightfoot, Transport Phenomena 2nd ed. (2007), John wiley & Sons, Inc. ISBN 978-0-470-11539-8

[12] E. L. Cussler, Diffusion : mass transfer in fluid systems third edition 2009, Cambridge University Press ISBN 978-0-521-87121-1

[13] F. Gabriel, G. Aiello, and J.-F. Salavy, A methodology to assess the impact of the manufacturing margins of the HCLL-TBM first wall in the design criteria, Fusion Engineering and Design 84 (2009) 798-803.

[14] S. Cho, M-Y. Ahn, D.W. Lee, Y-H. Park, E.H. Lee, et al., Design and R&D progres of Korean HCCR TBM, Fusion Engineering and Design xxx (2014) xxx-xxx, http://dx.doi.org/10.1016/j.fusengdes.2014.01.032.

[15] P. Chaudhuri, E.R. Kumar, A. Sircar, S. Ranjithkumar, V. Chaudhari, et al., Status and progress of Indian LLCB test blanket systems for ITER, Fusion Eng. Des. 87 (2012) 1009-1013.

[16] K.M. Feng, C.H. Pan, G.S. Zhang, T.Y. Luo, Z. Zhao, et al., Progress on design and R&D for helium-cooled ceramic breeder TBM in China, Fusion Eng. Des. 87 (2012) 1138-1145.

Ch. 2. Instability of the liquid metal column and droplet formation

Summary of this chapter

Formation of the Rayleigh mode droplet of liquid Li-17Pb released from a nozzle into vacuum was studied for the first step evaluation of the feasibility as a tritium extraction process. The size of droplets formed from the nozzles was estimated by theory and verified by the experimental methods. By the instability theory, the droplet diameter is described as an incredibly simple formula $d_{droplet} = 1.89 D_0$, *where* D_0 *is a diameter of the nozzle. By the non-dimensional comparison, above formula was confirmed to be applicable for the liquid Pb-17Li from the nozzle diameter 0.4mm to 1.0mm, temperature 400°C to 500°C, at initial velocity of 3 m/s. The experimental results agreed well with the above deduced formula. Observation of the droplet shape suggested that the spherical oscillation occurs on the droplet surface.*

2.1 Introduction

The authors have proposed a concept of high temperature liquid Pb-17Li blanket and a process for recovery of tritium to be extracted from liquid droplets by diffusion in a vacuum-sieve-tray as depicted in Fig.1 for example. The ratio of tritium which is released from a sphere droplet under diffusion limited condition as a function of time is described as the equation below. [1]

$$\frac{M_t}{M_\infty} = 1 - \frac{6}{\pi^2} \sum_{n=1}^{\infty} \frac{1}{n^2} \exp\left(-Dn^2\pi^2 t / a^2\right) \qquad (2.1),$$

where, t is diffusion time [sec]; a is radius of a droplet [m]; D is diffusion coefficient [m^2/sec].

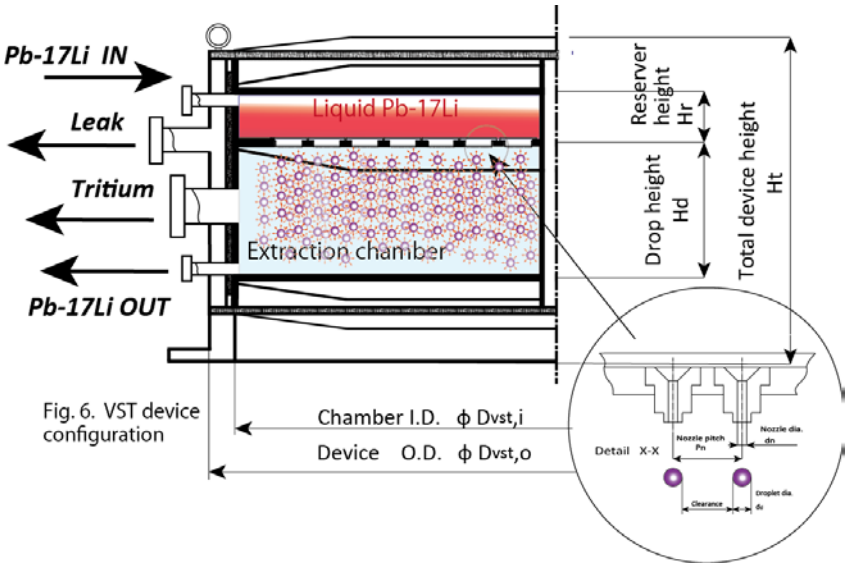

Fig.1 An example of the Vacuum-sieve-tray image

Tritium rich liquid Pb-17Li flows into the upper-chamber. While flowing through the nozzles, the liquid PbLi turns into droplets, and releases tritium into the vacuum while falling in the lower-chamber. The released tritium gas is collected for the fusion fuel. The liquid PbLi is collected at the lower chamber and circulated into the blanket.

It is easily seen that the radius of a droplet a plays a pivotal role contributing to the tritium extraction. In due course the formula which explicates the radius of a droplet by its nozzle is a key tool for the basic design of vacuum-sieve-tray. Yamamoto et al. [2] has reported an experimental result of liquid Pb-17Li droplet formation and observed its radius is 0.9mm by a nozzle of 1.0mm diameter. Succeeding this work, this study intends to deduce a formula which describes the relationship between a droplet size and the radius of nozzle of liquid Pb-17Li and compare with experiment.

2.2 Theory

The droplet size is deduced by the variational principle method and also by the normal mode wave instability method, and the same result is deduced by two methods.

2.2.1 Modeling of a droplet formation and governing equation

The theory for water droplet [3] is based on the assumption that the undulation of the

surface of liquid column is symmetrical to the z-axis and is described as

$$r = a + \alpha \cos kz \qquad (2.2),$$

where, as illustrated in Fig. 2,

k is wave-number defined by using wavelength λ [m] as $k = 2\pi/\lambda$ [1/m]

a is original liquid column radius [m].

α is amplitude of the surface undulation [m] at time t [sec] which is defined by using growth rate q [1/sec] and initial amplitude a_0 [m] as

$$\alpha = a_0 e^{qt} \qquad (2.3)$$

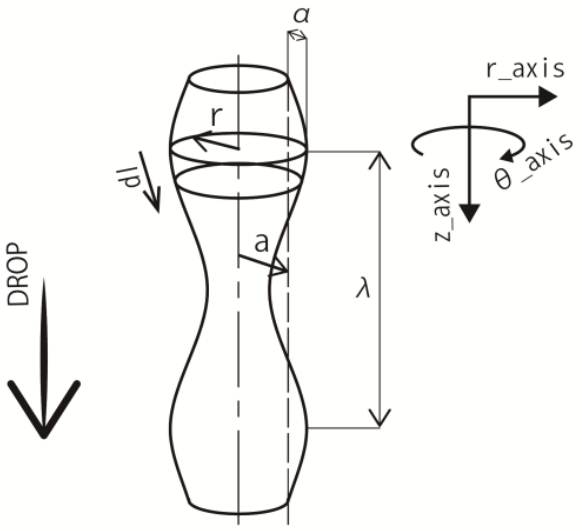

Fig.2 Coordinate system and notation diagram of droplet formation

And the deformation of liquid column is assumed to follow the surface energy minimizing condition. This condition is described by using a classic variational principle theory, namely Lagrange-Equation, as

$$\frac{\partial L}{\partial q}-\frac{d}{dt}\left(\frac{\partial L}{\partial \dot{q}}\right)=0 \tag{2.4},$$

where $L=T-U$ and T mean the kinetic energy and U is the potential energy respectively.

The potential energy of unstable column U with a wave number k is described by the difference of surface area and surface tension as

$$U=\sigma\left(s-s_0\right)=-\sigma\frac{\pi\alpha^2}{2a}\left(1-a^2k^2\right) \tag{2.5}$$

where σ is surface tension [N/m], $\left(s-s_0\right)$ is difference of surface area [m^2] between original cylindrical column and unstable column. Mathematical deduction detail is described in the Appendix-A.

The kinetic energy T is described as below by using the radial velocity potential ϕ which is derived from a non-compressible continuity condition. Mathematical deduction detail is described in the Appendix B.

$$T=\tfrac{1}{2}\rho\int_S 2\pi a\left(\phi\frac{\partial\phi}{\partial r}_{r=a}\right)dz=\tfrac{1}{2}\pi\rho a^2\frac{I_0\left(ka\right)\dot{\alpha}^2}{kaI_1\left(ka\right)} \tag{2.6}$$

where ρ is density [Kg/m^3], I_0 I_1 are modified Bessel's equation of zero and first order. [6]

By merging these results into equation and using a boundary condition, finally growth rate of the instability q is expressed as a function of only ka and has a real value under the condition $1\geq ka\geq 0$.

$$q^2=\frac{\sigma}{a^3\rho}\frac{\left\{1-\left(ka\right)^2\right\}\left(ka\right)I_1\left(ka\right)}{I_0\left(ka\right)} \tag{2.7}$$

2.2.2 Evolution of the unique wavelength and a droplet formation

The growth rate of the instability $\frac{q}{\sqrt{\frac{\sigma}{a^3\rho}}}$ written as a function of ka is shown in Fig.3-a.

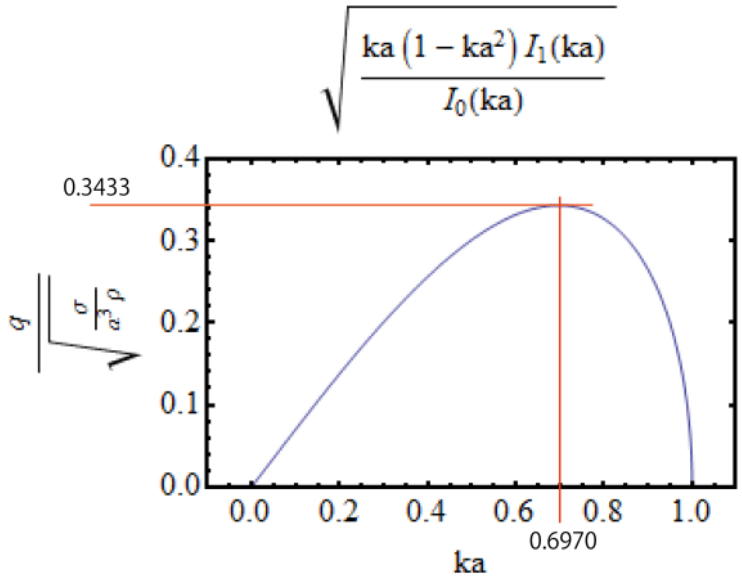

Fig.3-a. Growth rate *q* normalized vs. wave-number *ka*

It is seen that the growth rate q has a maximum at $ka \cong 0.697$ be maximum $q \cong 0.343\sqrt{\frac{\sigma}{a^3\rho}}$ then characteristic wavelength λ_1 is calculated as

$$\lambda_1 = \frac{2\pi}{k} \cong \frac{2\pi a}{0.697} \cong 9.0a \qquad (2.8)$$

This result shows that a wave of liquid column of one unique wavelength overwhelms the various surface undulations and finally grows up to form droplets. By this mechanism, the droplet size is calculated from the equal volume of one droplet and one wave-length λ_1 liquid column, i.e. $\frac{1}{6}\pi d_{droplet}^3 = \pi a^2 \lambda_1 \cong 9.0\pi a^3$.

Then droplet size is expressed by using a nozzle diameter $D_0 = 2a$ as a formula below.

$$d_{droplet} \cong \frac{(9.0 \text{x} 6)^{\frac{1}{3}}}{2} 2a = 1.89 D_0 \quad \text{[m]} \tag{2.9}$$

The characteristic time-constant of the growth of the instability t_{gr} is calculated by inversing the growth rate q as

$$t_{gr} = 1/q \cong \frac{1}{0.343\sqrt{\frac{\sigma}{a^3 \rho}}} \quad \text{[sec]} \tag{2.10},$$

in case of Pb-17Li droplet from a 1.0 mm diameter nozzle at 400°C, the characteristic growth time is 4.8 msec.

2.2.3 Verification of the theory applied for the liquid metal

Non-dimensional normal direction stress equilibrium equation between droplet and vacuum ambience is express as

$$-p_d' + \frac{1}{Fr} z' + \frac{2}{\text{Re}} \mathbf{n} \cdot \mathbf{E}' \cdot \mathbf{n} = \frac{1}{We} \nabla' \cdot \mathbf{n} \tag{2.11}$$

where

$Re = U_{ch} L_{ch} / \nu$ is “Reynolds number” ,

$Fr = U_{ch}{}^2 / g L_{ch}$ is “Froude number” represents Inertia vs. Gravity

$We = \rho U_{ch}{}^2 L_{ch} / \sigma$ is “Weber number” represents Inertia vs. Surface tension.

Comparison of these three characteristic parameters is shown in Table 1. It shows that liquid Pb-17Li at the temperature of 400°C to 500°C is in surface tension dominating phase and belongs to the same regime with that of water at 20°C. Then it is reasonable to presume both materials show similar behavior at temperature above mentioned so the equation for water droplet is applicable also for the liquid Pb-17Li droplet analysis. All bulk properties used for calculation is summarized in Table 1. [8]

Table 1. Comparison table of the normalized numbers

	Density	Viscosity	Surface tension	Temperature	Velocity	Length	Reynolds number	Froude number	Weber number
	ρ	μ	σ	T	U	L	Re	Fr	We
	Kg/m^3	$N\sec/m^2$	N/m	$Celsius$	$m/\sec$	m	UL/ν	U^2/gL	$\rho U^2 L/\sigma$
H_2O	$1.0x10^3$	$1.0x10^{-3}$	$0.7x10^{-1}$	20	3	$1.0x10^{-3}$	$3.0x10^3$	$9.2x10^2$	$1.3x10^2$
Pb-17Li	$9.7x10^3$	$1.5x10^{-3}$	$4.5x10^{-1}$	400	3	$1.0x10^{-3}$	$1.9x10^4$	$9.2x10^2$	$2.0x10^2$
Pb-17Li	$9.6x10^3$	$1.2x10^{-3}$	$4.4x10^{-1}$	500	3	$1.0x10^{-3}$	$2.5x10^4$	$9.2x10^2$	$2.0x10^2$

2.2.4 Effective range of the formula

The largest length considered by the above equations is defined as Froude number equals with Weber numbe*r* and it is described as

$$L_{chX} = \sqrt{\frac{\sigma}{\rho g}} \quad [\mathrm{m}] \tag{2.12}$$

In case of Pb-17Li at 400°C the critical length is calculated as 2.2mm and in case of water at 20°C it is 2.7mm.

2.2.5 Analysis by the wave instability theory

Above analysis was performed by the variational principle theory but it is also deduced by using the wave instability theory. [11] It assumes the infinitesimal wave fluctuation as

$$d = f\, e^{i\left(kz-\omega\tau\right)} \tag{2.13},$$

where *f, k,* ω is a non-dimensional amplitude of wave fluctuation, non-dimensional real wave number of z axis, and non-dimensional complex wave frequency, respectively. The ambient gas is vacuum and the liquid is assumed as inviscid. By using the conservation equations of momentum, mass and interfacial boundary condition, the dispersion relation is deduced as

$$\frac{I_0(k)(k-\omega)^2}{I_0'(k)}+\frac{k(1-k^2)}{We}=0 \qquad (2.14),$$

where I_0, I_0', *We* is the Bessel series function of *I(0)* and derivative of it, and the Weber number, respectively. The numerical calculation result has two results and one wave amplitude increases while the other decreases. It is shown at Fig. 3-b, which showed identical result with Fig. 3-a.

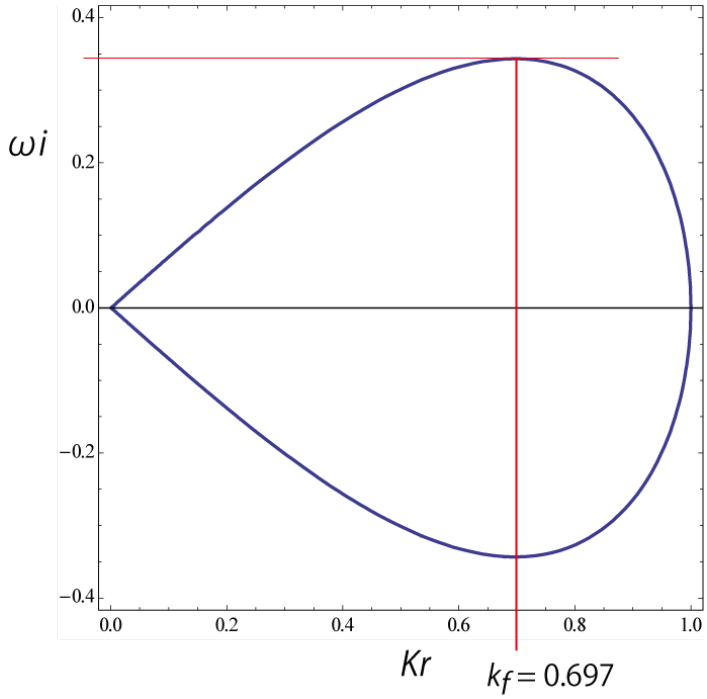

Fig. 3-b. Calculation result of the dispersion relation by using the wave instability theory.
The result has two results, one wave amplitude increases while the other decreases. It is identical with the Fig. 3-a which is performed on the variational principle theory.

2.3 Experimental

2.3.1 Experimental setup

A schematic of experimental setup is shown in Fig.4 and in Fig.5. It is consisted of a

reservoir, nozzles with various radii, sight windows, diffusion chamber, gas accumulation pump, vacuum pump and instruments.

Sizes are: the upper reservoir of ϕ150mm x100mm h, four nozzles with diameter from ϕ 0.4mm to ϕ 1.0mm, the lower diffusion-chamber of ϕ150mm x500mm h with observation windows. Deuterium and argon gas are supplied for the diffusion measurement. The nozzle is formed by drilling and finished for the Pb-17Li droplet and for the water formed injection needles were used. Chambers and nozzles were kept in temperature from 300°C to 500°C.

Diameter of the droplet was estimated from volumetric average and compared with photo. The volume of the dropped liquid was measured from a pressure difference in the upper chamber with the digital manometer-1 in Fig.4. Total number of droplets are measured by the high speed movie system VW-9000 of Keyence (4000 frames per sec.). Average diameter is calculated as it is a sphere shape, and its size variation and deviation from the sphere were observed from the photo images.

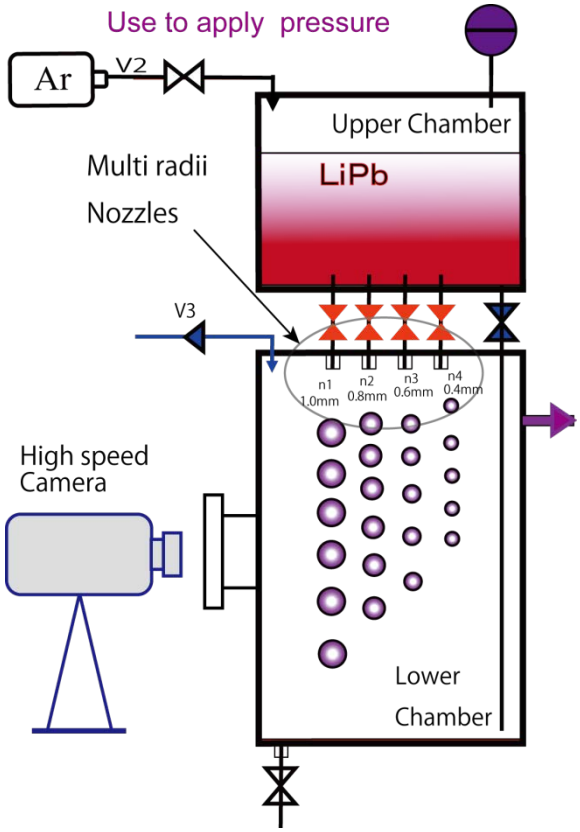

Fig.4 Schematic diagram of the experimental setup

Fig.5 Whole view of the experimental setup

2.4 Results and discussions

2.4.1 Observation of Pb-17Li liquid droplet formation

As shown in Fig.6, it was observed that the liquid Pb-17Li at 400°C drawn from the nozzle made a liquid column at first then only unique wavelength overwhelms the column surface and finally formed same size droplets. This complies with the theoretical analysis result.

Fig.6 Liquid column and droplets by 1.0mm dia. nozzle in a vacuum sieve tray

2.4.2 Measurement of droplet shape

Measured diameters of droplets along X and Y axis are shown in Fig.7 and Fig.8.

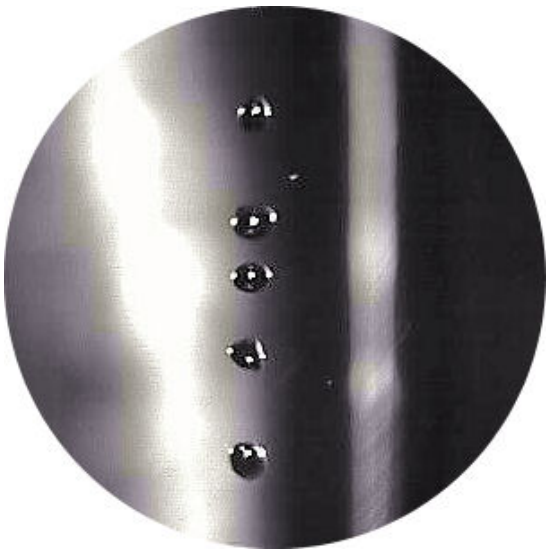

Fig.7 Droplets by 0.6mm nozzle

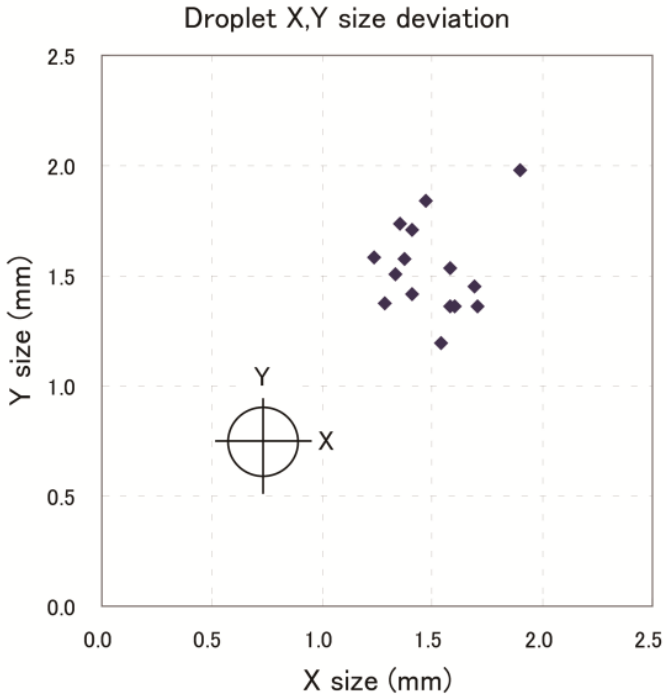

Fig.8 XY deviation of droplet diameter

The droplet shape was roughly sphere. The plots of the sphere shape, described as X and Y direction size on the Fig. 8, ranged from 0.7 to 1.3 suggested the spherical oscillation is occurring on the surface of the droplet.

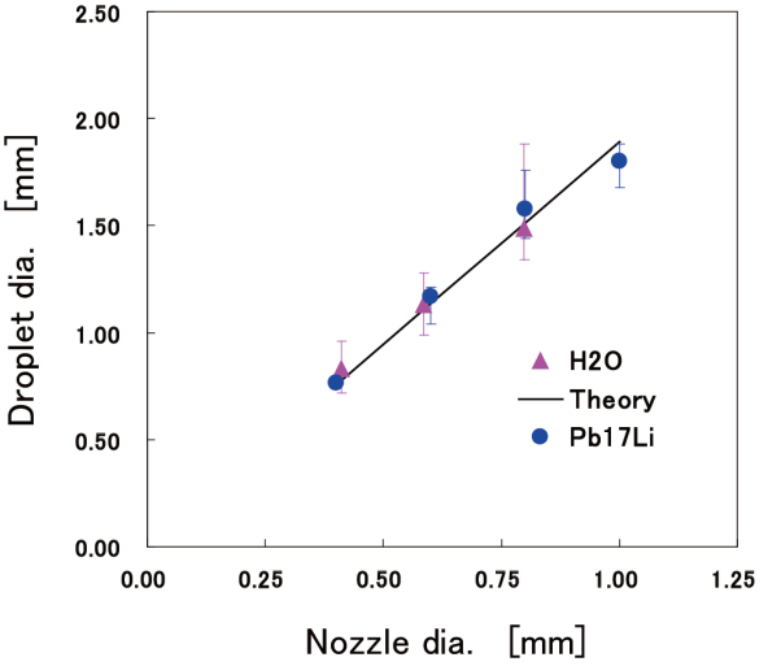

Fig.9 Experimental result of droplet diameter vs. liquid column
The observed droplet diameter of PbLi well accorded with the theory, while the nozzle diameter range of 0.4 mm to 1.0 mm, which is the surface tension dominating regime. As theory indicated, the diameter of the droplet is no relation with the density of the liquid media, and it is also shown on above chart.

2.4.3 Comparison with the theory

The measured droplet diameter of Pb-17Li at 400°C as a function of nozzle diameter, also droplet diameter of water at 20°C are shown in Fig.9.

In case of water, theoretical formula well describes the experimental result. In case of Pb-17Li, droplet diameter also agreed with the formula in a limited size region. At the nozzle diameter of 1.0mm resultant droplet size deviates 5% from the theoretical value to the smaller

side and it is presumed due to the influence of the effective range of this formula which is described by the equation(2.12). This result suggests that it can be used for the control of the size of liquid metal droplet by using prescribed nozzle size from which metal is extruded.

2.5 Conclusion

The formula to express the diameter of liquid Pb-17Li droplet is theoretically deduced by applying a surface minimizing theory and the wave instability theory. Under surface tension dominating regime, it is described only by using the nozzle diameter as $d_{droplet} \cong 1.89 D_0$, where D_0 is a nozzle diameter [m]. This formula was compared with the experimental results and it described the size of droplet Pb-17Li well. The observed droplet shape suggested that the spherical oscillation is occurring on the sphere surface. This result can be used for the vacuum-sieve-tray design by controlling the size of droplets in it.

Appendix A Difference of undulating surface area

Surface area of undulating column per length is

$$s_{un} = \frac{2\pi}{\lambda}\int_0^{\lambda} dl = \frac{2\pi}{\lambda}\int_0^{\lambda} r\left(1+\frac{1}{2}\left(\frac{dr}{dz}\right)^2\right)dz \simeq \pi a\left(2+\frac{1}{2}\alpha^2 k^2\right) \qquad \text{(AA1)}$$

Volume of undulating column per length is

$$v_{un} = \frac{\pi}{\lambda}\int_0^{\lambda} r^2 dz = \pi\left(a^2+\frac{\alpha^2}{2}\right) \quad \text{then} \quad a \simeq \sqrt{\frac{v_{un}}{\pi}}\left(1-\frac{\pi\alpha^2}{4v_{un}}\right) \qquad \text{(AA2)}$$

By AA1 and AA2 the difference of surface area per unit length $\left(s-s_0\right)$ is described as

$$\left(s-s_0\right) \simeq \frac{\pi\alpha^2}{2a}\left(a^2k^2-1\right) \qquad \text{(AA3)}$$

Appendix B kinetic energy by velocity potential

Velocity potential ϕ is defined as $v = \nabla\phi$ then kinetic energy T is described as

$$T = \frac{1}{2}\rho\int_V v^2 dV = \frac{1}{2}\rho\int_V (\nabla\phi)\cdot(\nabla\phi)dV$$

(AB1) and by using Green's first identity (AB1) is modified

$$\frac{1}{2}\rho\int_V (\nabla\phi)\cdot(\nabla\phi)dV = \frac{1}{2}\rho\int_S \phi\nabla\phi\cdot dS = \frac{1}{2}\rho 2\pi\int r\phi\frac{\partial\phi}{\partial r}dz \quad \because dS = 2\pi r dz \quad \mathbf{n}\cdot\nabla = \frac{\partial}{\partial r}$$

(AB2)

Due to continuity condition $\nabla^2\phi = 0$ ϕ is described as $\phi = A\mathrm{J}_0(ikr)\cos kz$

(AB3)

where $\mathrm{J}_0(x)$ is Bessel function of order zero. By AB2 and AB3 finally kinetic energy T is described $T = \frac{1}{2}\rho a^2\frac{\mathrm{I}_0(ka)\dot{\alpha}^2}{ka\,\mathrm{I}_0'(ka)}$, where $\mathrm{I}_0(x)$ is modified Bessel function or order zero.

References

[1] J. Crank, The Mathematics of Diffusion, Sec. 4, 6, Oxford University Press, ISBN 978-0-19-853411-2.

[2] Y. Yamamoto et al., Design of Tritium collecting system from LiPb dropping experiment, Fusion science and Technology Volume 60 Number 2 p558-562, Proceedings of the Nineteenth Topical Meeting on the Technology of Fusion Energy (TOFE) Part2 Aug. 2011

[3] Lord Rayleigh, On the instability of jets, Proceedings of the London mathematical society, Vol.10 1878, pp. 4-7

[4] S. Chandrasekhar, Hydrodynamic and Hydromagnetic Stability, Chapter X, Dover Publications, Inc. ISBN-10:0-486-64071-X

[5] Pierre-Gilles de Gennes et al., Capillarity and Wetting Phenomena Trans. by A. Reisinger, Sec. 5.2.4, Springer,

ISBN 0-387-00592-7 .

[6] M. Abramowitz et al., Handbook of Mathematical Functions, Sec. 9.6.27, Dover Publications, Inc, ISBN-10: 0-486-61272-4.

[7] Y.C. Fung, A first course in Continuum Mechanics Third Edition, Sec.7.3, Prentice Hall, ISBN 0-13-061524-2.

[8] E. Mas de les Valls et al., Lead-lithium eutectic material database for nuclear fusion technology, *J. Nucl. Mater.* **376** (2008) 353-357

[9] P. Calderoni et al., Measurement of hydrogen and deuterium solubility in the eutectic lead-lithium alloy, P3.90 Poster/Topic H : Fuel Cycle and Breeding Blankets: 25th SOFT Symposium on Fusion Technology, 15-19 Sept. 2008.

[10] F. Reiter, Solubility and diffusivity of hydrogen isotopes in liquid Pb-17Li, *Fusion Engineering and Design* **14** (1991) 207-211 North-Holland

[11] S.P. Lin, Breakup of Liquid Sheets and Jets, Cambridge University Press (2003), ISBN 0-521-80694-1

Ch. 3. Hydrogen isotopes mass transport on a falling liquid metal droplet

Summary of this chapter

The deuterium released by mass transport from falling droplets of Pb-17Li in vacuum was theoretically analyzed and verified by experimental. This prediction is one of key techniques of the tritium-extraction-device engineering design for the fusion reactor.

For the experimental of deuterium release, ambiguity of the deuterium solubility on liquid PbLi has annoyed many previous researchers. In this study, by comparing release amount from different diameter nozzles, ambiguous solubility problem is solved, and reliable result is attained. The resultant mass transport, represented by quasi dispersion-coefficient is 3.4 × 10^{-7} [m^2/s], which is approximately two orders of magnitude faster than previous studies under static condition. It also revealed different temperature dependency.

Theoretically deduced Sherwood number (ratio of dynamic mass transport and static diffusion) was between 494 and 598, and explained the experimental result of the two orders of magnitudes differences. These results show the falling droplets of liquid Pb-17Li in vacuum follow the mass transfer mechanism under convection prior domain by self-excited oscillation.

This result suggests that the tritium recovery method from a breeding liquid Pb-17Li blanket is viable when using multiple nozzles in vacuum for the extraction.

Notation

a	Radius of the droplet	[m]
c_{1i}	Concentration of solute #1 at the interface	[mol / m^3]
c_1	Concentration of solute #1 at the bulk	[mol / m^3]
$\mathcal{D}$	Diffusivity	[m^2/s]
$\mathcal{D}_{qua}$	Quasi dispersion coefficient; defined on this study as	[m^2 / s]
f_d	Natural frequency of droplet oscillation	[1/s]
$d_d(i)$	Diameter of the droplet from the nozzle(i)	[m]
k_d	Mass transfer coefficient	[m/s]
k	Mass transfer coefficient	[m / s]
$M^{de}(d_n(i))$	Amount of released deuterium from droplets through nozzle(i), while one falling period.	[mol]
$M^{LiPb}(d_n(i))$	Mass of Pb17Li droplets from a nozzle(i), while one measurement	[mol]
N_1	Flux of solute #1	[mol / m^2s]

$\mathfrak{S}$	Solubility	[mol / mol]
t_d	Dropping period of one Pb17Li droplet in VST	[s]

3.1 Introduction

We have proposed the use of a high temperature liquid Pb-17Li blanket and a process for recovery of tritium from falling liquid droplets by mass transport in a vacuum-sieve-tray (VST) device, as shown in Fig. 1 in Ch. 2. This device aims to extract dissolved tritium, from liquid Pb-17Li droplets, while the droplets are falling in vacuum.

The extraction ratio of tritium from the liquid Pb-17Li is a critical design parameter for the VST device. Many previous studies were performed to identify the hydrogen isotopes transport property of liquid Pb-17Li, ex., E. Mas de les Valls et al. [1], F. Reiter [2], and many other researchers. These previous measurements were performed under static condition, even though reported values were deviated approximately one order of magnitude. The main reason of deviation was assumed that measurements were affected by the ambiguous solubility condition.

Furthermore, a falling droplet in VST is moving, the mass transport is predicted to be enhanced due to the dynamic mechanism. Due to the unsteady-state transfer process of a falling droplet, many sophisticated studies of mass transfer from droplets have been performed mainly by numerical calculation.[3] On the other hand, for the proto-type design engineering of tritium extraction device, rather simple analytical Sherwood number and mass transfer coefficient of hydrogen isotopes from falling liquid Pb-17Li droplet in a short period, was requested but so far not established.

In this chapter, the mass transport of deuterium from falling liquid droplets of Pb-17Li is theoretically predicted. Then it was measured by experimental without the ambiguous solubility effects. Then the availability of simple criteria is validated for the mass transfer of deuterium extracted from falling droplets of liquid Pb-17Li in a vacuum. The contents of this chapter is mainly based on the previous papers. [4,5]

3.2 Theory

As described in Chapter 2, the oscillation of the droplet while falling is presumed to enhance the mass transport of dissolved hydrogen isotopes. In this section, the enhancement of the mass transport from an oscillating droplet is theoretically analyzed.

3.2.1 Analysis of the Droplet Oscillation

The frequency of cyclic deformation of a falling droplet from 0.6mm diameter nozzle was observed as approximately 200 [Hz]. Bulk properties of liquid Pb-17Li were examined by comparing the non-dimensional parameters that characterize the behavior of the falling droplet. As shown in Table 1 in Ch. 2, liquid Pb-17Li at temperatures between 400 °C and 500 °C is categorized as a typical Weber number dominated material, i.e., surface tension dominates the physical behavior of its motion. It is roughly one order greater than the gravity effects represented by the Froude number, and two orders greater than the viscosity effects represented by the Reynolds number. The natural frequency of a small liquid droplet under surface tension domain, is described by the following equation when surrounded by an infinite mass of another liquid

$$f_d = \frac{1}{2\pi}\sqrt{\frac{n(n+1)(n-1)(n+2)\sigma}{a^3\left[(n+1)\rho_d + n\rho_c\right]}} \tag{3.1}$$

where, **n** is a solid harmonics of **n**th degree and **n**=2 is the basic mode of oscillation.[5]

The calculated frequency of an n=2 basic mode oscillation is f_d=227.1 Hz, frequency of an n=3 mode oscillation is f_d=439.8 Hz. The modal deformation at n=2 is well known to have as an axisymmetric shape and a cyclic transition between spherical and vertically oblong and oblate, as schematically depicted in Fig. 1 [6].

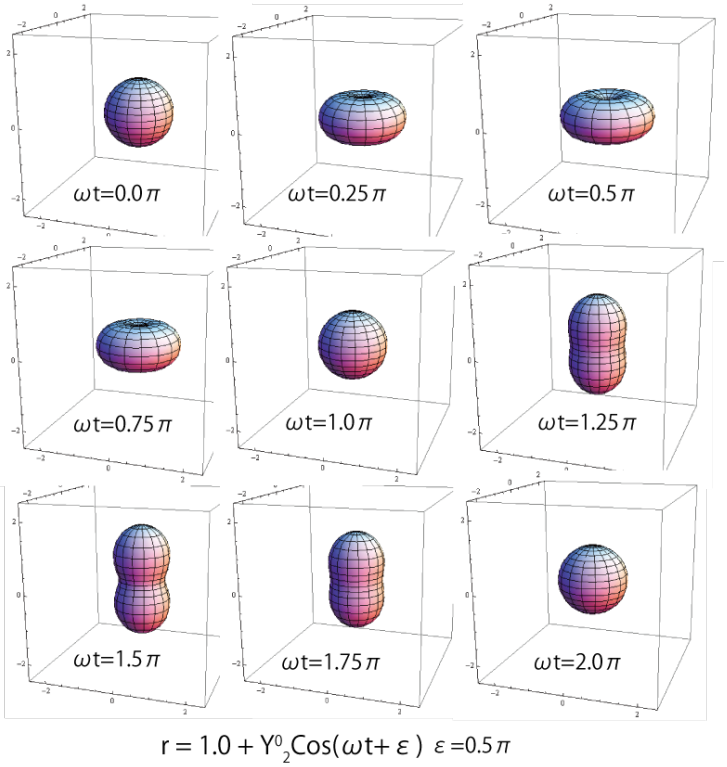

Fig. 1. Simulation model of modal deformation of a droplet, oscillating at basic mode (n=2) of natural frequency. It shows an axisymmetric deformation.

3.2.2 Mass Transfer Analysis of an Oscillating Droplet

The mass transfer theory of oscillating droplets by analytical methods, were summarized by A. Kumar and S. Hartland. [7] As to the mass transfer coefficient of an oscillating droplet under dispersive mode, two methods were introduced. One is a surface-stretch model.[8,9] The other is the new-surface-element model. [10] Each method was based on the different hypothesis, but the deduced results were close to each other. In this study, by the observation of the droplet oscillation, the results of the surface-stretch model were used. The basic hypothesis is closer to the observed results. By the works of Angelo et al., the mass transfer coefficient was described as

$$k_d = \sqrt{\frac{4\mathcal{D} f_d \left(1+\varepsilon+\frac{3\varepsilon^2}{8}\right)}{\pi}} \tag{3.2}$$

Corresponding Sherwood number is described from the definition as

$$S_h = \frac{k_d d_d}{\mathcal{D}} = \sqrt{\frac{4 f_d \left(d_d\right)^2 \left(1+\varepsilon+\frac{3\varepsilon^2}{8}\right)}{\pi \mathcal{D}}} \tag{3.3}$$

In this study, due to the droplets are falling in vacuum, the overall mass transfer coefficient is assumed same with mass transfer efficient of the droplet.

3.3 Experimental

3.3.1 Evaluation Criterion

Dynamic mass transport is considered, in general, a combination of diffusion and motion of fluid such as convection. Mass transfer coefficient and Sherwood number are commonly used to describe this transport phenomenon. But this falling droplet in VST, the experimental result was not well analyzed by previously developed criteria, due to the following reasons. Generally used analytical mass transfer coefficient is defined to describe the solute mass flux through the interface of a solvent as $N_1 = k\left(c_{1i} - c_1\right)$. The flux is assumed not so high, so the bulk concentration is regarded as constant. On this droplet case, the amount of mass transport is more than half of the total solute in a droplet, but not 100%, within a short dropping period of approximately 0.1 second. So bulk concentration is not constant, it must be analyzed as unsteady-state mass transfer. A simple analytical mass transfer coefficient to describe the release phenomenon of droplet in VST, is inherently difficult, and simple coefficient is not prevalent.[3]

To evaluate this experimental result by simple criterion, in this study, the concept of axial-dispersion-coefficient is introduced.

It was reported by G. Taylor [11] and modified by R. Aris [12]. A solute was introduced in a constant solvent flow within a tube over a very short period. The mass transport was theoretically studied by using the axial dispersion coefficient which has a same dimension with diffusivity coefficient of M^2/T. Solute in a flow was proved to follow the form of Fick's law equation. Different from the diffusion coefficient, this axial dispersion coefficient depends on

the flow velocity and diffusion coefficient.[13,14] Due to the short release period, and a solvent flowing with solute, the mass transport of deuterium from Pb17Li falling droplets, resembles with Taylor's precondition. So the concept of axial dispersion coefficient is applied to correlate the experimental results of falling droplets in a VST. To avoid confusion, in this study, the quasi-dispersion-coefficient, $\mathcal{D}_{qua}$ which has the same function with the axial dispersion coefficient, is used.

As it follows the Fick's law, the many previous analyses developed for the "diffusion" can be correlated with this study. Due to the dropping is in vacuum, and within a short period, the overall mass transport is assumed as equal with that of at the interface, in this study.

3.3.2 Experimental Setup and Measurements

A schematic and photograph of the experimental setup are shown in Fig. 2-a. and Fig. 2-b. respectively. This setup consists of a reservoir, nozzles with various radii, sight windows, the lower chamber, a gas accumulation pump, a vacuum pump and measuring instruments. Due to regulations, deuterium gas is used instead of tritium for this experiment.

The dimensions of the components are described as follows: the upper reservoir is ϕ150 mm × 100 mm height, the diameters of the four nozzles are 0.4 mm, 0.6 mm, 0.8 mm and 1.0 mm, and the lower chamber is ϕ150 mm × 500 mm height with observation windows. Deuterium and argon gas are supplied for the release measurements. The nozzles are formed by drilling and finished by wire-cut for the Pb-17Li droplet. The deuterium gas is supplied via valve V1 to the Pb-17Li in upper chamber and the soluble pressure is controlled by the digital manometer-1.

To examine the mechanism of mass transport, falling droplets were observed with a high speed movie camera, VW-9000 Keyence at 4000 [frames /s].

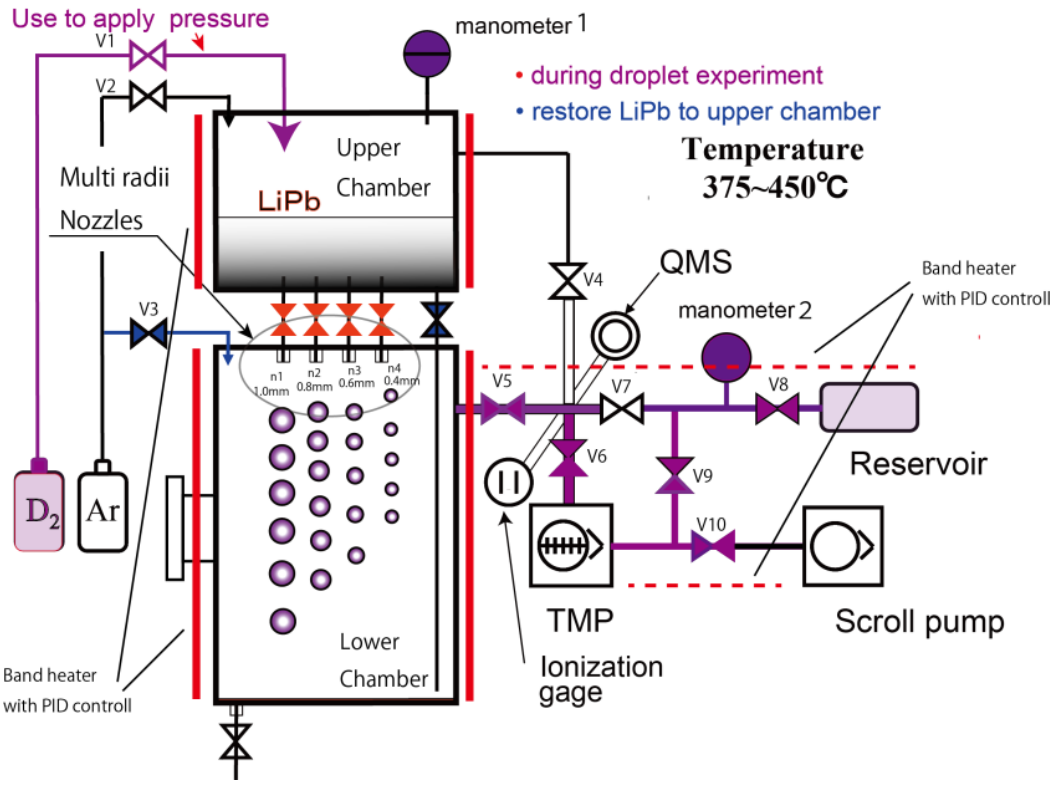

Fig. 2-a. Schematic of the experimental setup

Deuterium gas is well absorbed into Pb17Li at the upper chamber, released from falling droplets at the lower chamber in vacuum, in a short period of 0.1 second, and collected at the reservoir. Four different size nozzles are equipped to eliminate the solubility effect.

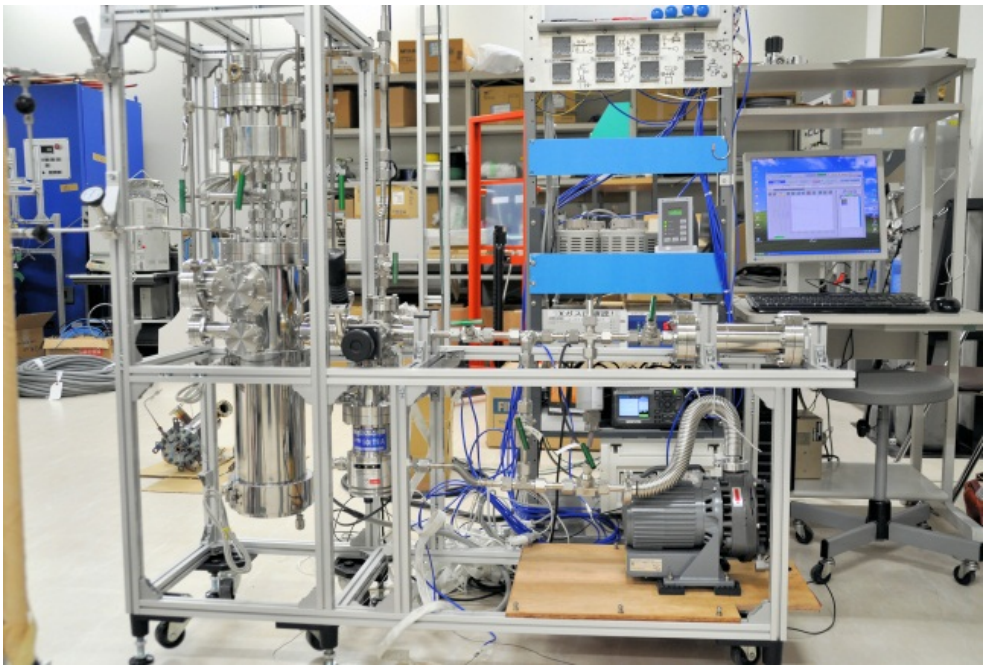

Fig. 2-b. Photograph of the experimental setup.
Heat insulators are removed for picture taking.

3.3.3 Amount of Released Deuterium

3.3.3.1 Precondition

The deuterium released from chain of droplets in a vacuum was accumulated into the reservoir through TMP. The amount of released deuterium was calculated by using the pressure reading on manometer-2, pre-measured reservoir capacity and temperature. The total volume of falling Pb-17Li droplets was calculated by using the pressure difference of upper chamber by manometer-1, with pre-measured capacity and temperature.

Heating was done with eight band type heater, each was independently temperature PID controlled. Experimental was performed under four different temperature conditions of 375 ºC, 400 ºC, 425 ºC and 450 ºC. Deviation of temperature after the equilibrium condition was within 2 ºC, by data logger monitor reading. Accumulated reservoir area, between V5 and reservoir of Fig. 2-a, was always kept at 120 ºC due to the temperature limitation of measurement devices.

The concentration of absorbed deuterium for the experiment was controlled by the policy that, at least within one set of experiments, which means one condition with four different nozzle drops, the concentration of deuterium must be same. Although absolute solubility was uncertain due to the effects of surfactants, progress of oxidization, etc., in longer periods. As

shown in Fig. 4, the deviation of released gas ratio was rather small, so above policy was believed to be effective. Detail procedures of absorption were as follows. a) The absorption time was fixed as 150 minutes for each experiment, which is 1.5 times that of pre-examined test result. The convection caused by the side heating was believed to reduce absorption time. b) Concentration difference of absorbed deuterium at the upper, middle and lower portion of the liquid Pb17Li in upper chamber was negligible, by the comparison of each released gas. The convection by side heating was also believed to enhance well dilution.

3.3.3.2 Released Deuterium Measurement

A measurement example is shown in Fig. 3. The horizontal axis is the duration time. The vertical axis is the pressure reading from the manometer-2. Both time and pressure are offset to zero at the start of dropping.

The pressure rise, which corresponds to the point < b > to < e > on Fig. 3 hereafter written as < b-e >, only occurred when falling droplets of Pb17Li were equilibrated with deuterium at upper chamber for the same long time. When the droplets were fallen without deuterium absorption (dry-run), no pressure rise occurred, and it showed just background level rise, same with < a-b >. By this pre-examination, the pressure rise < b-e > was confirmed by the deuterium absorption. It was also confirmed by QMS measurement.

The background gas while falling was regarded < b-c >, it is assumed as same rate with < a-b >.

The deuterium released from the deposition of Pb17Li at the bottom of lower chamber, corresponds < d-d' >, and continues to release while < d'-e > after falling stops. Number of droplets per one experiment condition is about 1×10^5, so the release rate is constant, it must be plotted as the linear line on the Fig. 3. The overshoot deviation from this linear line, which corresponds to < d-d' > is considered as the release from the deposition.

The net amount of deuterium, released while a falling period, correspond < c-d >, by removing the release from background and deposition.

Then, the measured extracted deuterium was rescaled with the following equation to obtain the atomic fraction of extracted gas per liquid Pb-17Li for non-dimensional evaluation.

$$E(d_n(i)) = \frac{M^{de}(d_n(i))}{M^{LiPb}(d_n(i))} \tag{3.4}$$

The measurement results for the extraction ratio $\boldsymbol{E(dn(i))}$ as a function of the nozzle diameter $\boldsymbol{dn(i)}$ at 450 ° C is shown in Fig. 4.

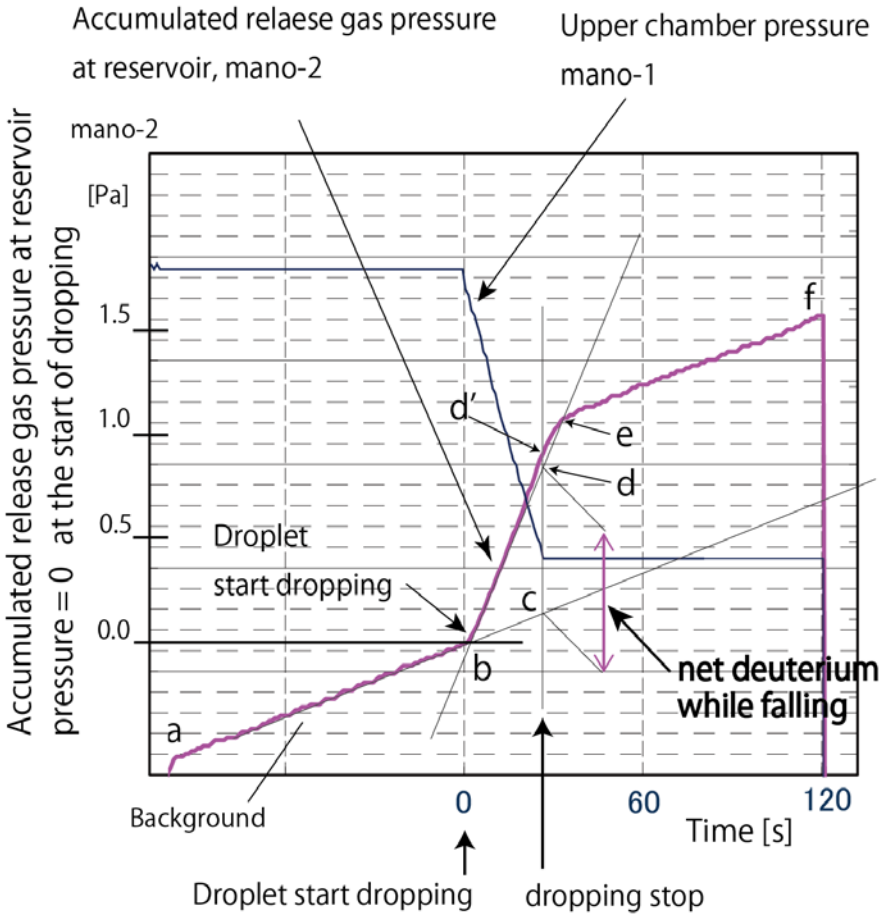

Fig. 3. An example of the accumulated released deuterium from chain of droplets,

measured as the pressure evolution at the reservoir. The upper chamber pressure is also plotted to specify the start and stop of dropping time. < c-d > is the net deuterium release from falling droplets, while falling. < b-c > is background gas while dropping period. < d-d' > is released gas from deposited Pb-17Li liquid at the bottom of lower chamber. Gas release from deposited Pb-17Li continues until < e >.

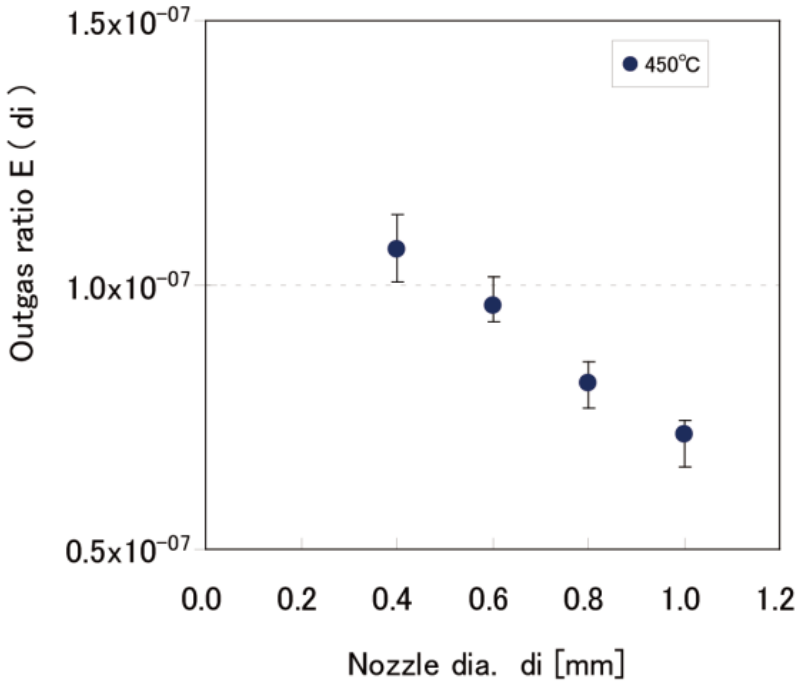

Fig. 4. Plots of normalized amount of released deuterium shown as atomic fraction, at 450 °C. The horizontal axis is the diameter of nozzles used for experiment.

3.3.4 Survey of Quasi Dispersion Coefficient

The amount of deuterium released from a droplet is described as the product of solution and release processes, and the theoretical extraction ratio is described as equation(3.5) under constant temperature, soluble pressure and dropping time conditions.

$$\mathcal{S} \cdot Th(\mathcal{D}_{qua}, t_d, d_n(i)) \tag{3.5}$$

As shown in above equation, to identify the reliable quasi dispersion coefficient, without the influence of ambiguous solubility, at least two different nozzle diameter data are required. To eliminate solubility, the function ***TTh*** which is defined as equation (3.6), is introduced. By dividing the numerator and denominator of each different diameter nozzle data under same soluble condition, solubility is eliminated. By this processing, the quasi dispersion coefficient is an only unknown parameter as shown below.

$$TTh(\mathfrak{D}_{qua}, d_n(i), d_n(j)) = \frac{\mathfrak{S} \cdot Th(\mathfrak{D}_{qua}, t_d, d_n(i))}{\mathfrak{S} \cdot Th(\mathfrak{D}_{qua}, t_d, d_n(j))} = \frac{Th(\mathfrak{D}_{qua}, t_d, d_n(i))}{Th(\mathfrak{D}_{qua}, t_d, d_n(j))} \quad (3.6)$$

The amount of deuterium released from a sphere droplet within a short period, can be described by using quasi dispersion coefficient as an equation (3.7) [15] based on the discussion at Sec. 3.2.1.

$$Th(\mathfrak{D}_{qua}, t_d, d_d(i)) = 1 - \frac{6}{\pi^2} \sum_{n=1}^{\infty} \frac{1}{n^2} \exp\left[\frac{-\mathcal{D}_{qua} n^2 \pi^2 t_d}{\left(d_d/2\right)^2} \right] \quad (3.7)$$

The function ***EE*** which divides each experimental result from the four different nozzles, is also defined as an equation below.

$$EE(d_n(i), d_n(j)) = \frac{E(d_n(i))}{E(d_n(j))} \quad (3.8)$$

By comparing of *TTh* to *EE* for the four different nozzles, if there is a unique quasi dispersion coefficient to fulfill following condition, it is the specific value of this experiment.

$$TTh\left(\mathcal{D}_{qua}, d_n(i), d_n(j)\right) = EE\left(d_n(i), d_n(j)\right) \quad (3.9)$$

To perform a complete parametric survey, the following equation is prepared,

$$Err(\mathcal{D}_{qua}) = \frac{1}{(16-4)} \sum_{i,j=1}^{4} \left(1 - \delta_{ij}\right) \left(\frac{EE\left(d_n(i), d_n(j)\right)}{TTh\left(\mathfrak{D}_{qua}, d_n(i), d_n(j)\right)} \right)^2 \quad (3.10)$$

where $\boldsymbol{\delta_{ij}}$ is the Kroenecker's delta and is used to eliminates the division with same data.

A parametric survey of the quasi dispersion coefficient was performed, and the survey results at 450 °C are shown in Fig. 5. The horizontal axis is the parametric value of quasi dispersion coefficient**,** and the vertical axis is the resultant error value of the parameter survey. For all four temperature cases ranging between 375 °C and 450 °C, the existence of a unique $\boldsymbol{D_{qua}}$ value was confirmed within 0.003 to 0.013 errors.

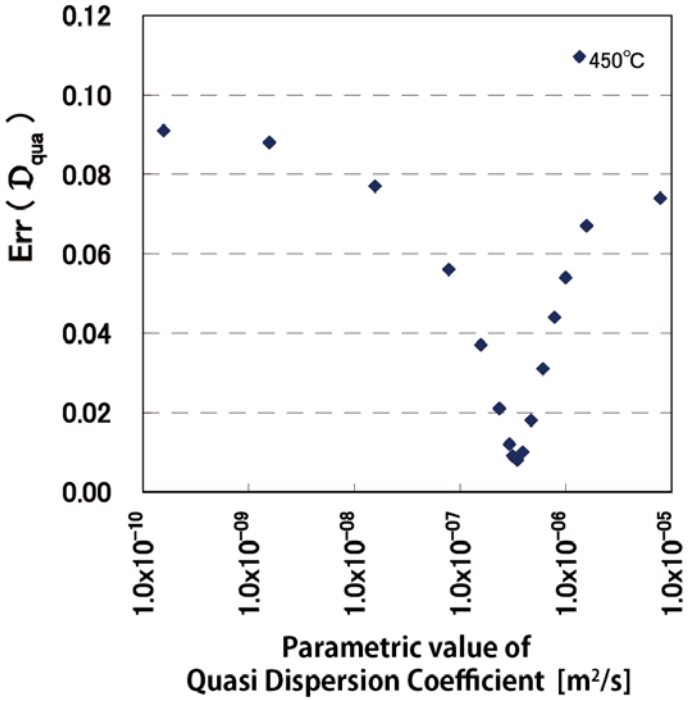

Fig. 5. Result of the parameter survey of quasi dispersion coefficient of deuterium

in falling Pb-17Li droplet at 450 °C. Horizontal axis shows the range of parametric survey value. Vertical axis is the corresponding error by Eq. (6). Unique value was determined as 3.4×10^{-7}.

3.3.5 Observation of Falling Droplets with a High Speed Movie Camera

As shown in Fig. 6, a cyclic deformation between a spherical-shape and an ellipsoidal-shape was observed for the falling droplet. The deforming frequency of a droplet from the 0.6 mm diameter nozzle was approximately 200 Hz. The amplitude of deforming radius was 13 % , and the size effect for mass transport was estimated between plus 7 % and minus 8 % by the calculation, so the effect of deformation from sphere can be neglected, due to the accuracy of this study.

Fig. 6, Oscillating deformation of one droplet,
recorded with high speed video camera. Frequency was approximately 200 Hz.

3.4 Results and discussions

3.4.1 Dispersion coefficient

From this experiment, the resultant quasi dispersion coefficient as a function of temperature is shown in Fig. 7, and a previously reported diffusivity example is plotted in the same chart for reference. The attained value was $\boldsymbol{D}_{\mathbf{app}} = 3.4 \times 10^{-7}$ [m^2/s] at 400 °C in this study, and was approximately three hundred times larger (1.2×10^{-9} [m^2/s]) in a study by Reiter.

The temperature dependency of this experiment showed less dependency than those of Reiter, which was described by an empirical equation $D = 4.03 \times 10^{-8} \exp(-19500/RT)$. The cyclic deformation, frequency of approximately 200 Hz, on the droplet was confirmed.

These results show the mass transport process, which includes convection and diffusion, also occur at the release of deuterium from falling liquid Pb-17Li droplets in a vacuum.

The elimination of the ambiguous solubility was well functioned by this method, considering the deviation of the attained results.

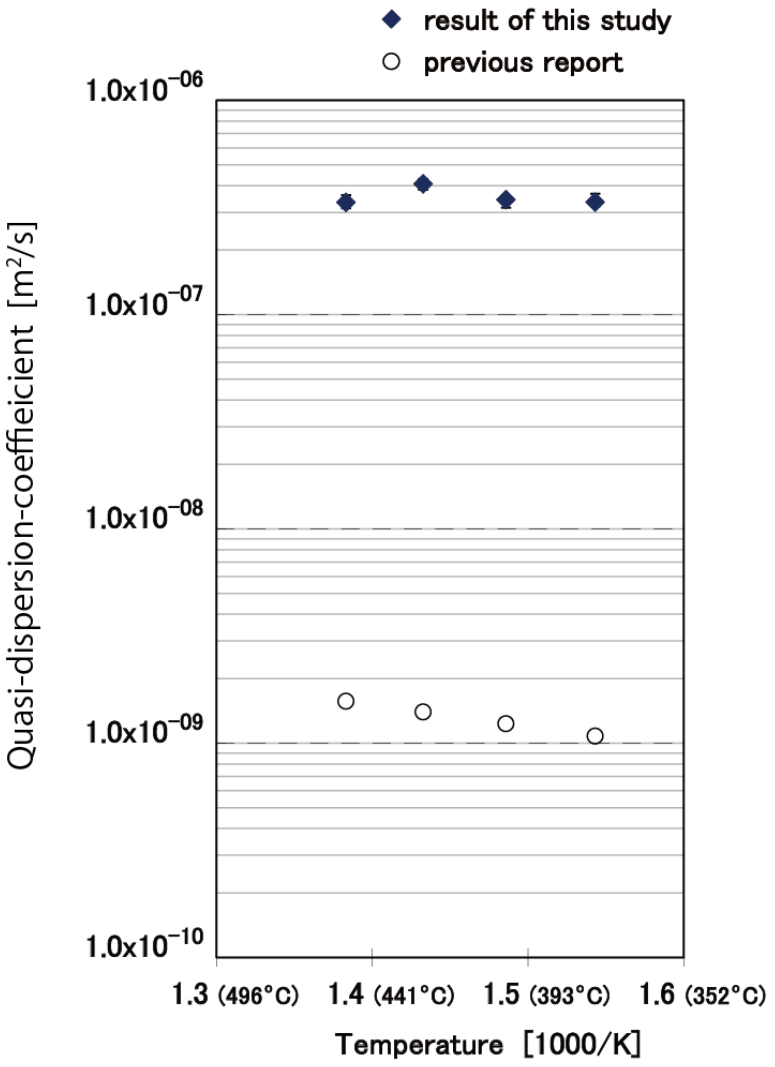

Fig. 7. Plots of the quasi dispersion coefficient of deuterium in the falling Pb-17Li droplets, versus the inverse of experimental temperature

The previously reported diffusivity values by Reiter are also plotted for reference. The attained results show two orders of magnitudes higher value. The less temperature dependency is considered that the convective prior mass flow also occurs in the Pb-17Li droplet.

3.4.2 Sherwood Number

As shown in Fig. 8, the Sherwood number for oscillating droplets and the experimental results are plotted in the same chart. The vertical axis shows the Sherwood number, and the horizontal axis shows the reciprocal the temperature. Experimental is performed under four different temperatures of 375 ºC, 400 ºC, 425 ºC and 450 ºC. A surface stretch ratio is assumed ε=0.1 in all four droplet size, due to the resolution limit of high-speed recordings, significant difference was not distinguished.

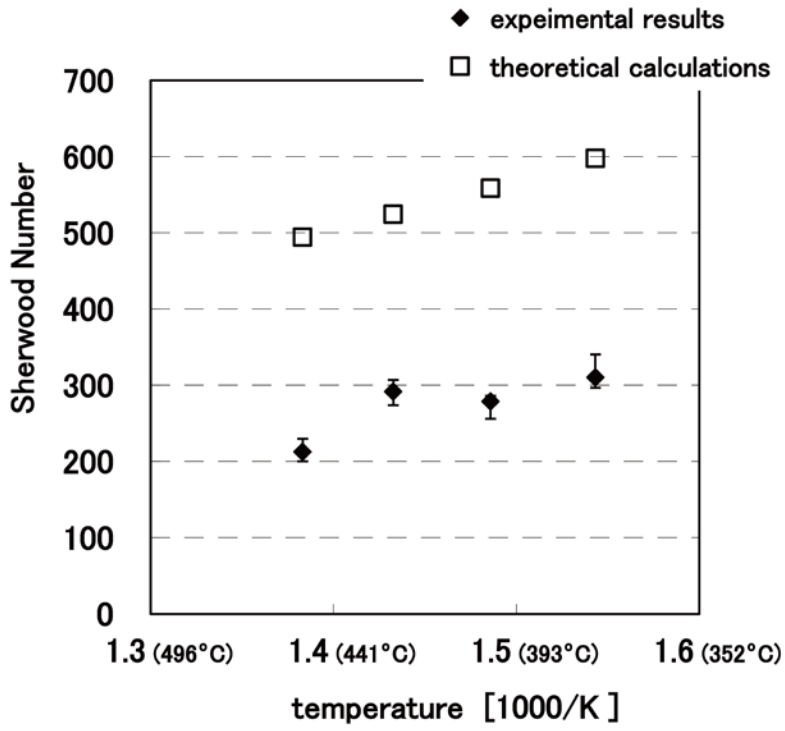

Fig. 8. Plots of theoretical Sherwood numbers compared with experimental results.
Horizontal axis is reciprocal the temperature, vertical axis is Sherwood number.

As shown in Fig. 8, theoretically calculated Sherwood numbers and corresponding experimental results were plotted on the same chart. Theoretical Sherwood numbers were between 494 and 598. The experimental results were between 213 and 310. This result explained the two orders of magnitudes difference of the deuterium mass transport from falling droplets. Temperature dependency showed good accordance with each other. Though, the ratio of theory and experimental still remain between 1.8 and 2.3.

3.4.3 Discussions

The theoretical Sherwood number showed 1.8 to 2.3 times higher than the experimental result. It is considered as follows.

a) The amount of solute in a droplet is finite. The concentration of the solute in a droplet must decrease by each emission, but it is not taken into account to deduce the equation. The corresponding boundary condition, $c = c_0|_{y=0,\, t>0}$ [107,108] which means the concentration on the stretched surface is always same with the beginning, does not reflect the true situation of a falling droplet in vacuum. So theoretically deduced result dully shows higher value, and it is as shown in Fig. 2.

b) The number of deformation cycle within one droplet falling time, is not taken into account. Total amount of release must depend on the number of emission, but it is not considered. This also decreases the experimental result.

c) The diffusivity value reported by previous studies has larger deviation, possibly due to the difference of the measurement method.[2,3] This affects the calculation.

The other errors and uncertainty on the parameters such as viscosity due to the Li-Pb contents, or radius of the droplets can also be the reason for the discrepancy. They could also affect the result but it is presumed to be rather small compared with above three items.

3.5 Conclusion

The released deuterium from the falling liquid droplets of Pb-17Li in vacuum was theoretically analyzed, and experimentally measured without the ambiguous effects of solubility. Experiments were performed to compare different diameter nozzle data, to eliminate solubility effects. The mass transport of deuterium in Pb-17Li droplet, represented by quasi dispersion coefficient, was identified as $\boldsymbol{D_{qua} = 3.4 \times 10^{-7}}$ [m^2/s] at 400 °C. It is two orders of magnitude faster than the previous studies of under static condition. The attained results had less temperature dependency than previous studies.

The theoretical Sherwood number was between 494 and 598, and explained the two orders of magnitudes faster mass transport phenomenon. Though, the ratio of theory and experimental still remain between 1.8 and 2.3.

To attain a better prediction, an analytical model which include more realistic boundary condition, the number of droplet oscillation while falling, or accurate diffusivity values will be required. However for the practical purpose, the agreement is in a reasonable level for this kind

of very simple model, for understanding and taking into account the movement of liquid metal in fusion devices.

This result suggests that the tritium recovery method from the breeding liquid Pb-17Li blanket and VST device is viable.

References

[1] E.MAS DE LES VALLS, L.A.SEDANO, L.BATET, I.RICAPITO, A.AIELLO, O.GASRALDI, F.GABRIEL, "Lead-lithium eutectic material database for nuclear fusion technology," *Journal of Nuclear Materials*, **376**, 353-357 (2008).

[2] F. REITER, "Solubility and diffusivity of hydrogen isotopes in liquid Pb-17Li," *Fusion Engineering and Design*, **14**, 207-211 (1991).

[3] M. A. WAHEED, M. HENSCHKE, A. PFENNI, "Mass transfer by free and forced convection from single spherical liquid drops," *Int. Jour. Heat and Mass Transfer,* **45,** (2002) 4507-4514.

[4] F. Okino, K. Noborio, R. Kasada, S. Konishi, Enhanced mass transfer of deuterium extracted from falling liquid Pb-17Li droplets, Fusion Science and Technology, Vol. **64** Number 3 (2013), Pages 543-548.

[5] F. Okino, K. Noborio, R. Kasada, S. Konishi, Deuterium Transport Prediction in Oscillating Liquid Pb-17Li droplet, Fusion Science and Technology, Vol. **64** Number 3 (2013), Pages 549-551.

[6] H. LAMB, *Hydrodynamics 6TH ed.*, DOVER PUBLICATIONS, New York, (1932), pp.475, ISBN-10:0-486-60256-7.

[7] A. KUMAR, S. HARTLAND, "Correlations for prediction of mass transfer coefficients in single drop systems and liquid-liquid extraction columns," *Trans I. Chem. E.*, Vol. **77**, Part A, July 1999.

[8] P. M. ROSE, R. C. KINTNER, "Mass Transfer from Large Oscillating Drops", *A. I. Ch. E. journal*, Vol.**12**, No3 p530-534, 1966.

[9] J. B. ANGELO, E. N. LIGHTFOOT and D. W. HOWARD, "Generalization of the Penetration theory for Surface Stretch: Application to Forming and Oscillating Drops", *A. I. Ch. E. Journal,* Vol.**12** No.4 page 751-760, 1966.

[10] R.J. BRUNSON, R.M. WELLEK, "Mass Transfer Within Oscillating Liquid Droplets," *Can. J. Chem. Eng.*, **48**, (1960), 267-274.

[11] G. TAYLOR, "Dispersion of soluble matter in solvent flowing slowly through a tube," *Proc. Roy. Soc.,* **A219**, 186-203 (1953).

[12] R. ARIS, "On the dispersion of a solute in a fluid flowing through a tube," *Proc. Roy. Soc.*, **A235**, 67-77 (1956).

[13] R.B. BIRD, W.E. STEWART, E.N. LIGHTFOOT, *Transport Phenomena* 2nd , PP. 643-646, John Wiley & Sons, Inc., ISBN 978-0-470-11539-8.

[14] E.L. CUSSLER, *DIFFUSION MASS TRANSFER IN FLUID SYSTEMS*-3rd ,2009, PP. 95-107, CAMBRIDGE UNIVERSITY PRESS, ISBN 978-0-521-87121-1.

[15] J. CRANK, *The mathematics of diffusion. -2nd ed.*, pp.89–91, OXFORD UNIVERSITY PRESS, Oxford , U.K. (1979). ISBN 978-0-19-853411-2.

Ch. 4. Tritium recovery device design for ITER scale fusion reactor

Summary of this chapter

This study proposes a practical design for a tritium extraction device. A liquid Pb-17Li blanket and a vacuum-sieve-tray extraction device are employed in the design. The practical tritium extraction ratio achieved with the proposed device is 0.35. The inner chamber of the extraction device is 2.5 m in diameter and 0.25 m high with a one-stage configuration. The device is sufficient for the fuel supply of an ITER class fusion reactor with the assumptions of a smooth supply of tritium to the plasma chamber. These results reveal a significant reduction in size from devices proposed in previous studies and provide a wider range of design allowances.

Subscripts & Superscripts

*	time variable
PL	Pb-17Li
tr	tritium
dt	d + t reaction
nl	n + lithium reaction
b	blanket
x	stockpile
c	core

Notations

ϕ Tritium extraction constant in blanket loop [1/s] $\phi = \frac{Q_{PL}}{V_{PL}}\left(\frac{M_t}{M_\infty}\right)$

ε_b Tritium leak constant in blanket loop [1/s]

ε_x Tritium leak constant in stockpile [1/s]

λ_{tr} Tritium decay constant [1/s]

$A_0 = R_{dt,c}\left(B_{tr} - 1\right)$

$A_1 = -R_{dt,c}\, B_{tr}$

$A_2 = \left(\lambda_{tr} + \varepsilon_x\right)$

A_b Surface area of the blanket loop [m^2]

A_x Surface area of the stockpile [m^2]

B_{tr} Tritium breeding ratio [-]

$$C_0 = N_0 - \frac{A_0}{A_2} - \frac{A_1}{(A_2 - \phi)} = N_0 - \frac{R_{dt,c}(B_{tr} - 1)}{(\lambda_{tr} + \varepsilon_x)} + \frac{R_{dt,c} B_{tr}}{(\lambda_{tr} + \varepsilon_x - \phi)}$$

$C_{tr,\mathrm{b}}$ Concentration of tritium in a blanket loop [mol/m^3]

$C_{tr,x}$ Concentration of tritium in a stockpile [mol/m^3]

$\mathscr{D}_{tr,x}$ Diffusivity of tritium at the stockpile wall [m^2/s]

$\mathscr{D}_{tr,\mathrm{b}}$ Diffusivity of tritium at the blanket loop wall [m^2/s]

$D_{vst,i}$ Inner diameter of the VST for the nozzle plate [m]

D_x Diameter of the stockpile [m]

d_d Diameter of the droplet [m]

d_n Inner diameter of the nozzle [m]

g Gravity [m/s^2]

H_d Dropping height in a VST [m]

H_x Height of the stockpile [m]

J Tritium leak flux from the stockpile wall [mol/m^{2}s]

J_b Tritium leak flux from the blanket loop wall [mol/m^{2}s]

$\mathrm{k_d}$ Droplet diameter coefficient [--] $\mathrm{k_d} = 1.89$

$\mathrm{k_p}$ Nozzle pitch coefficient [--]

$\left[\frac{M_t}{M_\infty}\right]$ Tritium extraction ratio during the finite period t versus infinite time [-]

M_t Amount of tritium transported between time zero and a time " t " [mol]

M_∞ Amount of tritium transported between time zero and infinity [mol]

N_0 Initial tritium inventory in the stockpile [mol]

N_n Total number of nozzles in the VST [-]

$N^*_{tr,b}$ Tritium inventory in the blanket loop [mol]

$N^*_{tr,x}$ Tritium inventory in the stockpile loop [mol]

$N^*_{tr,\Sigma}$ Total tritium inventory [mol]

p_n Nozzle pitch [m] $p_n = \mathrm{k_p}\, d_d$

Q_{PL} Flow rate of Pb-17Li in the blanket loop [m^3/s]

Q_{vst} Flow rate of Pb-17Li in the VST [m^3/s]

q_n Volumetric flow per nozzle [m^3/s]

$R_{dt,c}$ d + t reaction rate in the core [mol/s]

S_n Surface area per nozzle [m^2]

$S_{\Sigma n}$ Total area for the nozzles [m^2]

t_d Falling time for a droplet in a VST [s]

v_0 Initial velocity of the Pb-17Li droplet [m/s]

V_{PL} Volume of the Pb-17Li in a blanket loop [m^3]

V_b Inner volume of the blanket loop [m^3]

V_x Inner volume of the stockpile [m^3]

w_b Wall thickness of the blanket loop [m]

w_x Wall thickness of the stockpile [m]

4.1 Introduction

This paper proposes a practical design of a tritium recovery process for the liquid Pb-17Li blanket. Tritium is extracted from droplets falling in a pumped vacuum chamber by a continuously operated vacuum-sieve-tray (VST) device.

Mass transfer from droplets was previously believed to follow a static diffusion process. A multi-stage cascade extraction process was estimated as necessary to attain a designated sufficiently low concentration of tritium, and device size was an issue [1-4]. However, the authors report that the mass transport of deuterium from falling droplets was two orders of magnitude faster than expected [5]. After this result, the design allowances for the tritium extraction process were greatly relaxed.

Many previous studies have analyzed the tritium extraction and fuel-cycle of a liquid Pb-17Li blanket. These studies can be categorized into three groups. One group considered tritium permeation, safety issues, and extraction efficiency. The least necessary tritium extraction ratio was discussed based on the allowable released amount [6-17]. The second group considered the inventory of tritium. The least necessary tritium extraction ratio was discussed based on tritium self-sufficiency [18-21]. The third group of studies focused on the extraction method, device size, and efficiency which is the approach taken in this study [22-24].

However, the practical extraction ratio, which defines a quantity that is sufficient but not excessive, was not clarified by previous studies. The practical extraction ratio is a necessary constraint to the design of prototypes. This study aims to produce a practical design for a tritium extraction device based on a smooth supply of tritium. In the model design, a liquid Pb-17Li blanket and a VST extraction device are used.

4.2 Tritium extraction ratio

4.2.1 Analysis methods

In this study, the extraction ratio of an on-line VST device is considered assuming the smooth supply of tritium to the plasma chamber.

Another key factor to affect the extraction ratio is the permeation and release of tritium. It is a safety issue even on the order of ppm. However, according to the ITER TBWG tritium release guidelines [25], fifty times the annual amount of operation release is predicted in uncertain periods, and may leak from uncertain positions in the case of accidents. Thus, a decontamination factor greater than fifty is minimally required. A secondary enclosure and dedicated tritium collection devices are mandatory. The efficiency of an on-line extraction device affects only a small portion of the capacity of such a secondary tritium collecting devices. Therefore, in this study, permeation is not factored into the design of an on-line tritium extraction device.

4.2.2 Modeling of a tritium loop

The plant-lay-out model, which was first used by G. Veredas et al. [21], was retrofitted to accommodate this study. Although this model is extremely simple, it is suitable for clarifying the basic behavior of tritium inventory transition, which is an appropriate level of consideration for this study.

A schematic diagram of the plasma chamber, blanket, VST device, tritium stockpile, and two tritium loops used in this study is shown in Fig. 1. Liquid Pb-17Li is used as a blanket medium, and tritium is bred in the blanket. Then, the tritium-rich liquid Pb-17Li is circulated to an external VST device. While passing through the VST, tritium gas is extracted from the droplets by the mass transfer process, and the gas is stockpiled for re-supply to the plasma.

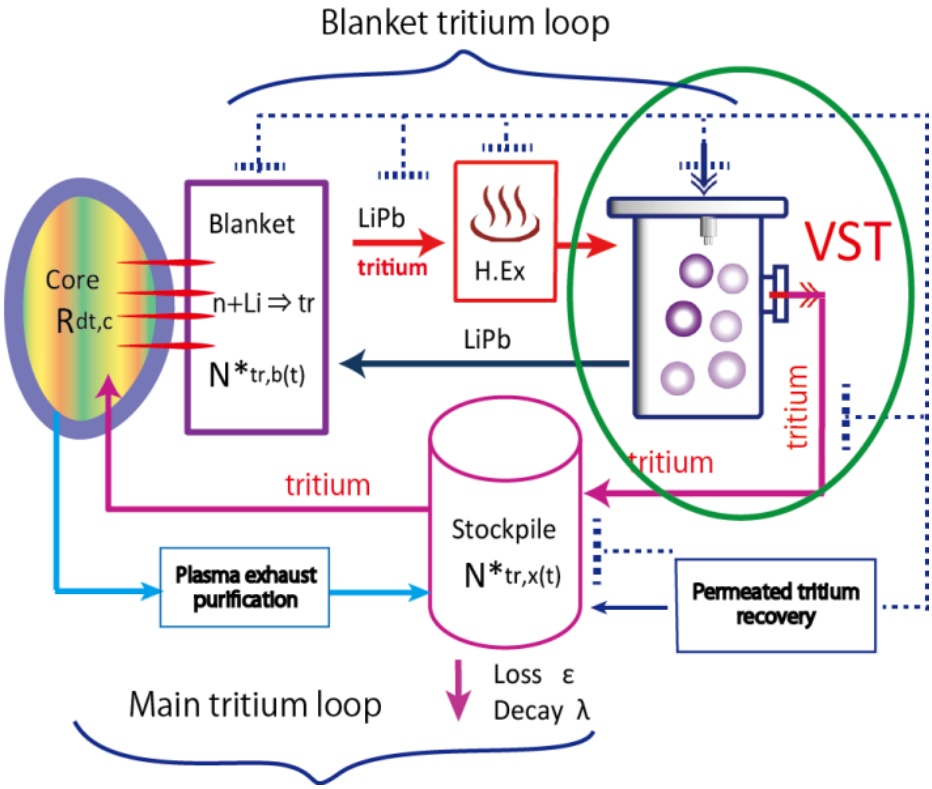

Fig. 1. A schematic of a fusion reactor system model.

The dissolved tritium in liquid Pb-17Li, which is bred in the blanket, is circulated between the blanket and the Vacuum-Sieve-Tray(VST). At VST, the dissolved tritium is released by mass transfer mechanism while droplets of PbLi are falling in vacuum. Droplets are formed by multi nozzles located at the top of VST. The collected tritium is stocked and re-fueled into the fusion core. The liquid PbLi is re-circulated into the blanket.

4.2.3 Tritium inventory in the blanket loop

The mass balance equation of the tritium inventory in the blanket loop can be described as below [26]. All notations are listed at the top of this chapter.

$$\frac{dN_{tr,b}^{*}}{dt} = B_{tr}R_{dt,c} - \left(\phi + \varepsilon_x + \lambda_{tr}\right)N_{tr,b}^{*} \tag{4.1}$$

Here, ϕ represents the tritium extraction constant in the blanket loop and plays a pivotal role in this equation. It is described by the following equation.

$$\phi = \frac{Q_{PL}}{V_{PL}}\left(\frac{M_t}{M_\infty}\right) \tag{4.2}$$

By short recycling time of Pb-17Li in the blanket tritium loop, and numerical comparison results, the order of magnitudes of the three constants $\phi, \varepsilon_x, \lambda_{tr}$ are $\phi >> \varepsilon_x >> \lambda_{tr}$, as described at the Appendix-A. Then hereafter, ε_x and λ_{tr}, i.e., leak constant and decay constant, are neglected and only ϕ, tritium extraction constant, is taken into account on the blanket tritium loop. In case of the leak constant is not negligible to the tritium extraction constant, i.e. $\phi \approx \varepsilon_x$, following discussions are less reliable and must be performed with the modified equation (4.1).

The resultant inventory equation for the blanket loop is described by using the initial condition $N^*_{tr,b}|_{t\to 0} = 0$. Details of the mathematical procedures are described at Appendix-B.

$$N^*_{tr,b} = \frac{B_{tr} R_{dt,c}}{\phi}\left(1 - e^{-\phi t}\right) \tag{4.3}$$

From equation (4.3), we can see that the tritium inventory in the blanket displays monotonous positive behavior.

4.2.4 Tritium inventory in the main tritium loop

The mass balance equation of the tritium inventory in the main tritium loop can be described based on a mass balance equation, as shown below:

$$\frac{dN^*_{tr,x}}{dt} = A_0 + A_1 e^{-\phi t} - A_2 N^*_{tr,x} \tag{4.4}$$

Here, $\boldsymbol{A_0}$, $\boldsymbol{A_1}$, and $\boldsymbol{A_2}$ are constants defined in the Notation section. The resultant inventory equation for the main loop is described by using the initial condition $N^*_{tr,x}|_{t\to 0} = N_0$. Details of the mathematical procedures are described at Appendix-B.

$$N^*_{tr,x} = \frac{A_0}{A_2} + \frac{A_1}{\left(A_2 - \phi\right)} e^{-\phi t} + C_0 e^{-A_2 t} \tag{4.5}$$

4.2.5 Inventory depression ratio

The stockpiled tritium inventory, described by equation (4.5), displays complicated behavior. To analyze this behavior, the time derivative is used, as shown below.

$$\frac{\partial N^{*}_{tr,x}}{\partial t} = \frac{A_1 \phi}{(\phi - A_2)} e^{-\phi t} - C_0 A_2 e^{-A_2 t}$$

The first term of the derivative is always negative because $\phi > A_2 > 0$ and $0 > A_1$. In contrast, the sign of the second term depends on the start-up tritium inventory.

When the device starts up with a small amount of initial tritium, which is preferable for fuel self-sufficiency, the derivative is first negative and then positive. This implies the existence of a minimum inventory depression.

A large depression of the stockpiled inventory must affect the smooth operation of the plasma-chamber. To evaluate this damage, the following depression ratio is defined. Here, zero implies no depression and a perfectly smooth supply of tritium, and 1.0 implies that tritium is out of stock and plasma is distinguished.

$$\left(\frac{\Delta N}{N_0} \right) = \frac{N_0 - N^{\min}_{tr,x}}{N_0}$$

4.2.6 Practical extraction ratio

To perform the case study, following key figures are assumed based on the report by Ichinose et al. [4, 28].

Fusion reactor specifications

Fusion output	P_{fus}	763	[MW_t]
Tritium consumption	$R_{dt,c}$	4.5×10^{-1}	[mol/s]
Breeding ratio	B_{tr}	1.05	
Flow rate of Pb-17Li	Q_{PL}	7.24×10^{-1}	[m^3/s]
Total volume of Pb-17Li	V_{PL}	3.19×10^{2}	[m^3]

VST case study results

Tritium extraction ratio		0.35	
VST inner diameter	Dvst,i	2.5	[m]
Droplet falling height	H_d	0.25	[m]
Nozzle diameter	dn	0.6×10^{-3}	[m]
Quantity of nozzles	Nn	4.2×10^{5}	
Initial velocity	v_0	3.0	[m/s]

Equivalent dispersion **D** 3.4×10^{-7} [m^2/s]

The result of a parametric survey is shown in Fig. 2. The size of the extraction device and the investment of the device roughly follow the extraction ratio. Extraction ratios greater than 0.35, marked as region < d > in Fig. 2, lead to a less efficient device. Thus, an extraction ratio of 0.35, marked as region < c >, is the practical upper limit of the device.

The validity of a depression ratio of 0.28 in region < c > depends on the robustness of the fuel supply system, which is unknown here and is therefore regarded as being at an acceptable level in this study. The details of the calculation are summarized in Sec.4.1. The tritium inventory time transition with a practical extraction ratio of 0.35 is shown in Fig. 3.

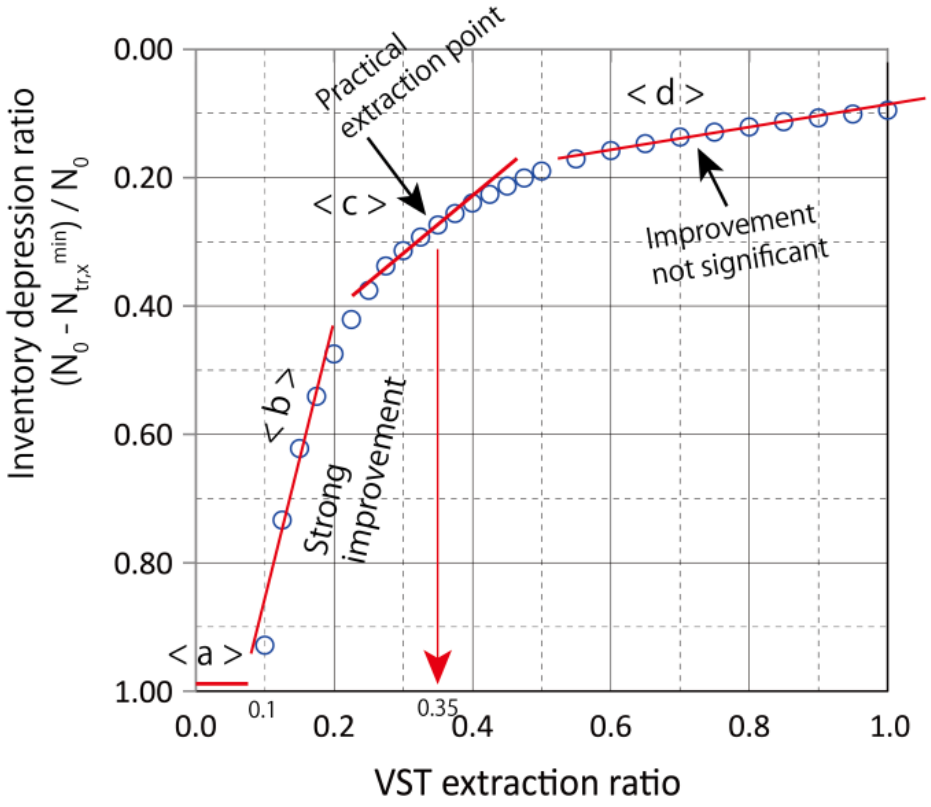

Fig. 2. Plots of the inventory depression ratio as a function of the VST extraction ratio.

Region < a >; Tritium inventory is out of stock.
Region < b >; Inventory depression is greatly improved by an increase of the VST extraction ratio.
Point < c >; Practical extraction point; Improvement of the depression is weakened beyond this point.

Region < d >; Improvement of the depression is not significant.

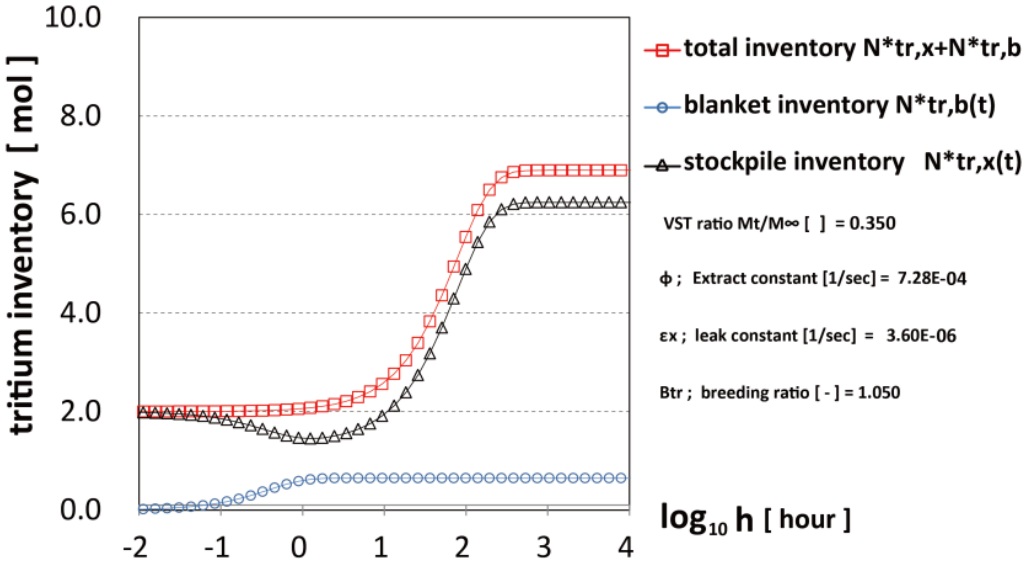

Fig. 3. Plots of the tritium inventory time transition with a practical extraction ratio of 0.35.

Triangular, round, and square shapes show the stockpile, blanket, and total inventory, respectively. The horizontal axis shows the hours after start-up on a logarithmic scale.
The minimum stockpiled inventory exists approximately two hours after start-up. The depression of the inventory at this minimum point primarily depends on the extraction ratio of the VST.

4.3. Design Theory for the VST

The configuration of the VST and details of its nozzle section are shown in Fig. 4-a and Fig. 4-b.

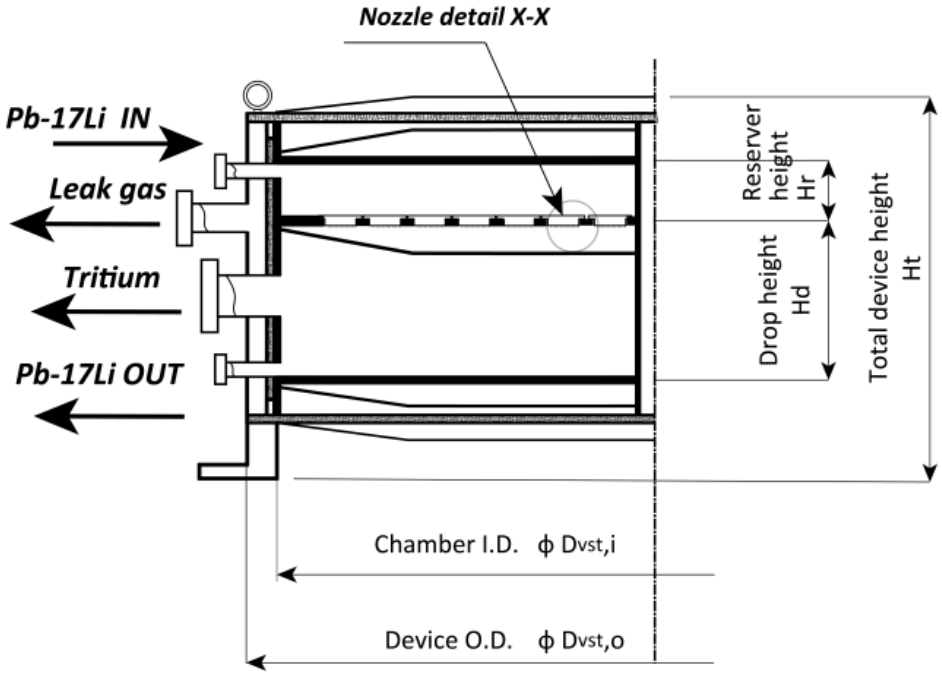

Fig. 4-a. VST device configuration

Tritium rich liquid Pb-17Li flows into the upper-chamber, flows through the nozzles, turns into droplets, and releases tritium into the vacuum while falling into the lower-chamber.

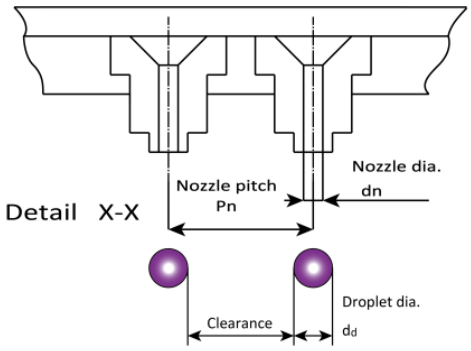

Fig. 4-b. Cross sectional view of the nozzles that generate the Pb-17Li droplets.

4.3.1 Required inner diameter for the VST extraction chamber

The inner diameter of the extraction chamber was determined through the following procedure.

The total number of required nozzles N_n was expressed by equation (4.6).

$$N_n = \frac{Q_{vst}}{q_n} = \frac{Q_{vst}}{\frac{\pi}{4} {d_n}^2 v_0} \tag{4.6}$$

The center pitch between adjacent nozzles ***Pn*** was defined as the product of the droplet diameter d_d and the pitch-coefficient ***kp***, as shown in equation (4.7).

$$p_n = k_p d_d = 1.89 k_p d_n \tag{4.7}$$

The pitch-coefficient ***kp*** is a design parameter that maintains clearance between falling droplets. The coefficient of 1.89 is a theoretically deduced relationship between the droplet and the nozzle diameter [27].

The area per nozzle ***Sn*** is defined as the square of the pitch-length in equation (4.8). Then, the total area required for all nozzles ***SΣn*** is described by equation (4.9).

$$s_n = {p_n}^2 \tag{4.8}$$

$$S_{\Sigma n} = s_n N_n = \frac{\left(1.89 k_p\right)^2 Q_{vst}}{\frac{\pi}{4} v_0} \tag{4.9}$$

The inner diameter of the VST ***Dvst,i*** is determined by equation (4.10).

$$D_{vst,i} = \sqrt{\frac{4}{\pi} S_{\Sigma n}} = 2.4 k_p \sqrt{\frac{Q_{vst}}{v_0}} \tag{4.10}$$

4.3.2 Required height for the VST extraction chamber

The minimum dropping time ***td*** that fulfills the required extraction ratio described in Sec. 2.6 was determined with the pre-calculated chart for a given quasi-dispersion-coefficient **D** and a given nozzle diameter, as shown in Fig. 5. After the minimum dropping time was fixed, the required height of the VST was calculated with equation (4.11) for a given initial dropping velocity v_0.

$$H_d = \frac{1}{2} g {t_d}^2 + v_0 t_d \tag{4.11}$$

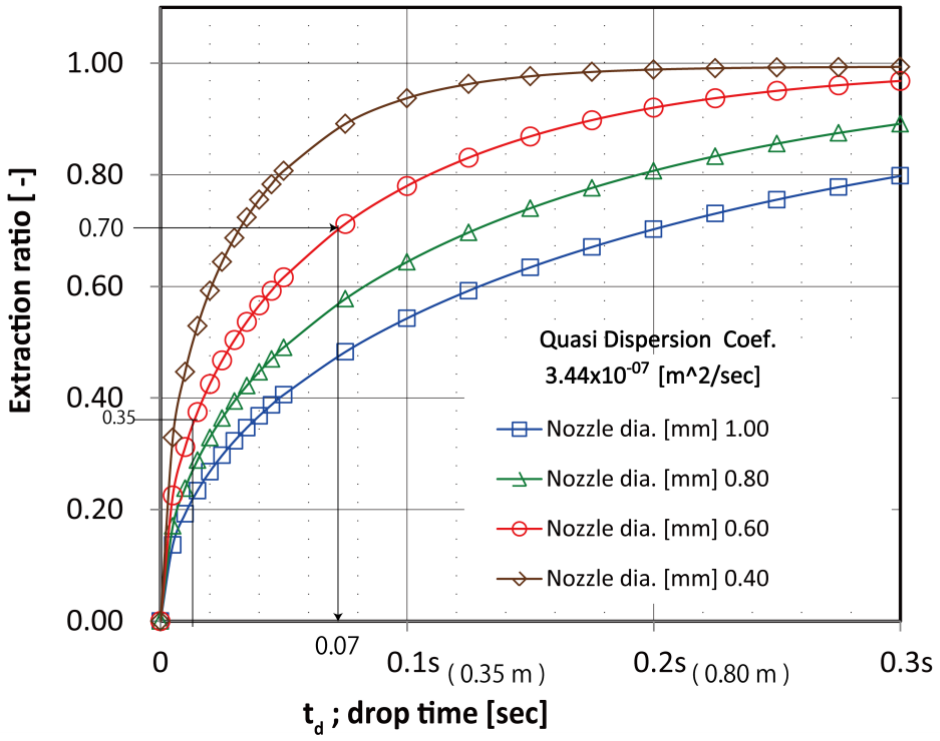

Fig. 5. Extraction ratio of tritium from a falling droplet in vacuum as a function of the drop period and nozzle diameter
The extraction ratio of tritium from a falling droplet is calculated with four different diameter nozzles, with initial velocity of 3 m/s. The vertical axis is the extraction ratio of tritium while falling. The horizontal axis is the falling period, corresponding falling height is also scaled.
From the safety point of view, the extraction ratio of tritium should be as high as possible. But secondary tritium extraction system is mandatory due to the permeation and unexpected release, so this primary loop of tritium extraction, the reasonably appropriate extraction ratio should be selected. In this case, falling period of 0.07 s, i.e., 0.3 m height, and the extraction ratio of 0.7 is selected for device design case study.

4.3.3 Case study

A case study of the VST prototype design was performed. As described in Sec. 2.6, the practical extraction ratio was 0.35.

From Fig. 5, the drop period required to extract 35% of the tritium was determined to be less than 0.03 sec, which is too short. Therefore, instead of using the full Pb-17Li flow, an extraction ratio of 70% with half of the Pb-17Li flow was used.

The inner diameter of the VST extraction chamber is 2.5 m. The dropping height was 0.25 m. The number of required nozzles is Nn= 4.2 × 10^5. Here, a nozzle pitch coefficient of ***kp*** =3 was adopted such that the clearance was twice the droplet diameter.

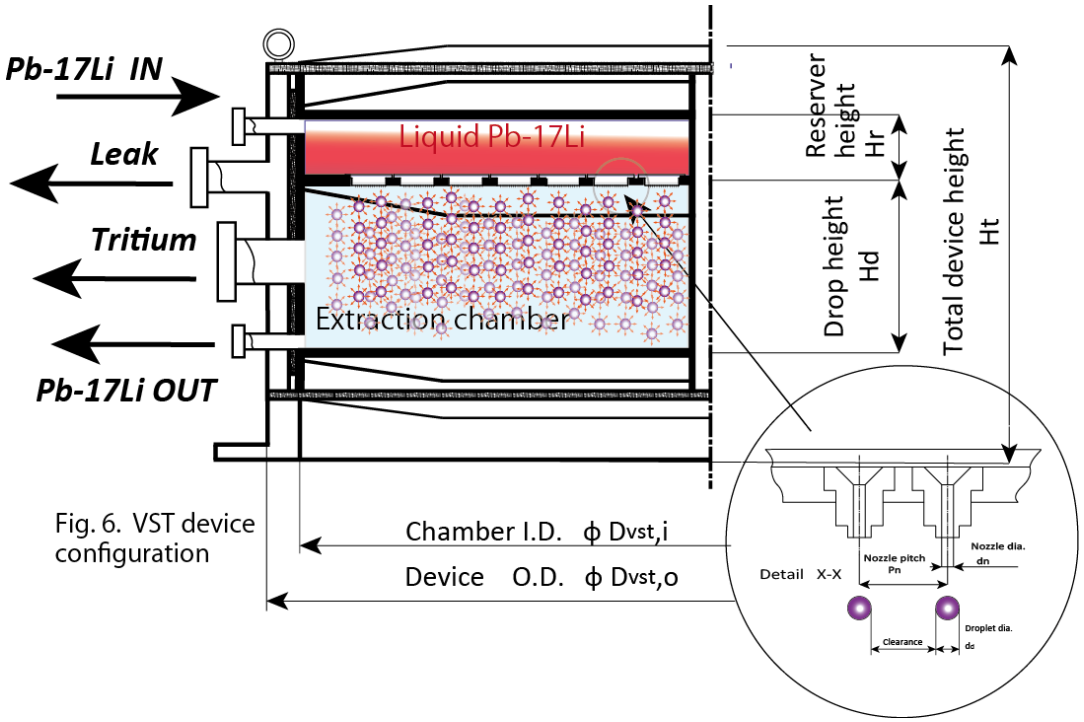

Fig. 6. VST device configuration

Fig. 6. Extraction device design model

The model used for the case study is depicted. Tritium rich liquid PbLi is supplied to the top of device. By flowing through the nozzles, liquid PbLi turns into droplets. The dissolved tritium is released while the droplets are falling in vacuum at the lower chamber. At the bottom of the lower chamber, the liquid PbLi is collected and turn back to the blanket system.

By a case study of ITER class fusion reactor, the inner diameter of the VST extraction chamber is 2.5 m and the dropping height is 0.25 m. This device size is comparable with the helium bubble extractor device size as Pierini described in his paper[6], and proved that the droplet extractor is reasonable device for the tritium extraction from liquid PbLi.

This case study is based on the high PbLi flow model, in case of low flow model like EU-HCLL, the device size is considered further smaller.

4.4 Results and Discussion

4.4.1 Results

The case study results for the VST device present smaller values than those of previous reports [1-4]. The practical tritium extraction ratio achieved with the proposed device is 0.35. The inner chamber of the extraction device is 2.5 m in diameter and 0.25 m high with a one-stage configuration. The device is sufficient for the smooth supply of tritium for an ITER class fusion reactor.

The faster hydrogen isotope mass-transfer from the oscillating Pb-17Li droplets, contribute to these smaller value results. [5]

4.4.2 Discussion

An enormous quantity of nozzles (4.2×10^5) is required, but this number is not a final figure. A design review of the nozzle shape is required during the engineering stage.

4.5 Conclusions

A method to determine the practical dimensions of a tritium-extracting device (VST) with a liquid Pb-17Li blanket was studied analytically.

In this case study of an ITER class fusion reactor, the practical tritium extraction ratio used was 0.35. The inner diameter of the extraction chamber was 2.5 m, and the dropping height was 0.25 m with a one-stage configuration. These results reveal significantly smaller resulting values than those of previous studies.

The behavior of tritium inventory in the main loop is the primary factor used to determine the practical extraction ratio. In particular, the depression of inventory at the minimum point and the efficiency of extraction improvements were analyzed to maintain the smooth supply of tritium. These results will contribute to the design of a prototype of the Pb-17Li blanket.

Appendix-A Comparison of the $\phi, \varepsilon_x, \lambda_{tr}$; tritium extraction constant, tritium leak constant in the blanket tritium loop, and tritium decay constant.

The typical tritium leak flux in a blanket loop is represented by following approximate one dimensional tube model as follows,

$$J_b = -\mathscr{D}\frac{dC_{tr,b}}{dx} = \mathscr{D}\frac{1}{w_b}\left(\frac{N_{tr,b}}{V_b}\right) \tag{4.12}$$

where x axis is defined as a tube wall thickness direction. Then the typical tritium leak constant in a blanket loop is deduced by following equation.

$$\varepsilon_b = \frac{J_b A_b}{N_{tr,b}} = \frac{\mathscr{D}_b A_b}{w_b V_b} \tag{4.13}$$

The leak constants of the stockpile is also deduced with same process.

By the parameters in Sec. 4.2.6, the tritium leak constant is $\varepsilon_b \simeq 1.0\times10^{-6}$ [1/s].

The tritium extraction constant $\phi = \frac{Q_{PL}}{V_{PL}}\left(\frac{M_t}{M_\infty}\right)$ is $\phi = 4.7\times10^{-4}$ [1/s].

The tritium decay constant $\lambda_t = \frac{\ln(2)}{T_{1/2}} = 1.8\times10^{-9}$. Then the condition $\phi >> \varepsilon_x >> \lambda_{tr}$ is satisfied.

Appendix-B Solution of the first order linear differential equation

The solution of the following first order linear differential equation

$$\frac{dy}{dt} + P(t)\,y = Q(t) \tag{4.14}$$

is known as

$$y = e^{-\int P(t)dt}\left[\int Q(t)e^{\int P(t)dt}dt + c\right] \tag{4.15}. [29]$$

Applying this theorem to the equation (4.1) after neglecting the leak and decay constant,

$$\frac{dN^*_{tr,b}}{dt} = B_{tr}R_{dt,c} - \phi N^*_{tr,b}$$

$P(t)$ and $Q(t)$ is assigned as

$$P(t)=\phi \ \vdots \ Q(t)=B_{tr}R_{dt,c},$$

then equation (4.1) is solved as

$$y=e^{-\int \phi dt}\left[\int B_{tr}R_{dt,c}e^{\int \phi dt}dt+c\right]=e^{-\phi t}\left[\frac{B_{tr}R_{dt,c}e^{\phi t}}{\phi}+c\right] \qquad (4.16)$$

By using the boundary condition $y\,|_{t\to 0}=0$, final solution is as

$$y=\frac{B_{tr}R_{dt,c}}{\phi}\left(1-e^{-\phi t}\right) \qquad (4.17)$$

The equation (4.4)

$$\frac{dN^{*}_{tr,x}}{dt}=A_0+A_1e^{-\phi t}-A_2N^{*}_{tr,x}$$

is solved with same process. In this case, $P(t)$ and $Q(t)$ is assigned as

$$P(t)=A_2 \ \vdots \ Q(t)=A_0+A_1e^{-\phi t}.$$

Inserting these results into the equation (4.15), the result is described as

$$y=e^{-\int A_2dt}\left[\int\left(A_0+A_1e^{-\phi t}\right)e^{\int A_2dt}dt+c\right]=e^{-A_2t}\left[\int\left(A_0+A_1e^{-\phi t}\right)e^{A_2t}dt+c\right]$$
$$=e^{-A_2t}\left[\left(\frac{A_0}{A_2}e^{A_2t}+\frac{A_1}{A_2-\phi}e^{(A_2-\phi)t}\right)+c\right]$$

(4.18)

By using the boundary condition $y\,|_{t\to 0}=N_0$, it is finally solved as equation (4.5)

$$N^{*}_{tr,x}=\frac{A_0}{A_2}+\frac{A_1}{\left(A_2-\phi\right)}e^{-\phi t}+C_0e^{-A_2t}$$

References

[1] G. Pierini, F. Massetti and C. Rizzello, Feasibility study of tritium recovery systems from 83Pb17Li breeding material of a D-T fusion reactor, Fusion technol. (1984) 463.

[2] C. Malara, G. Pierini and A. Viola, The feasibility of tritium extraction units from blanket of fusion reactors in the light of recent experimental data, Fusion Technol. (1992) 1429.

[3] H. Moriyama, S. Tanaka, D.K. Sze, J. reimann and A. Terlain, Tritium recovery from liquid metals, Fusion Eng. Des. 28 (1995) 226-239.

[4] Y. Yamamoto et al., "Design of Tritium collecting system from LiPb dropping experiment", Fusion science and Technology Volume **60** Number 2 p558-562, Proceedings of the Nineteenth Topical Meeting on the Technology of Fusion Energy (TOFE) Part2 Aug. 2011.

[5] F. Okino, K. Noborio, R. Kasada, S. Konishi, "Enhanced mass transfer of deuterium extracted from falling liquid Pb-17Li droplets," Fusion Science and Technology Vol. **64** Number 3 (September 2013) pages 543-548.

[6] W. Farabolini, A. Ciampichetti, F. Dabbene, M.A. Fuetterer, L. Giancarli, G. Laffont, et al., Tritium control modeling for a helium cooled lithium-lead blanket of a fusion power reactor, Fusion Eng. Des. **81** (2006) 753-762.

[7] I. Ricapito, A. Ciampichetti, G. Benamati, Tritiium management in HCLL-DEMO blanket, ENEA report LB-G-R-008, 2004.

[8] I. Ricapito, A. Aiello, A. Ciampichetti, G. Benamati, M. Utili, M. Zucchetti, Tritium management in HCLL-PPCS model AB blanket, Fusion Eng. Des. **82** (2007) 2195-2203.

[9] O. Gastaldi, N. Ghirelli and F. Gabiel, Tritium transfers and main operating parameters impact for demo lithium lead breeding blanket (HCLL), Fusion Eng. Des. **83** (2008).

[10] A. Li Puma et al., Breeding blanket design and systems integration for a belium-cooled lithium-lead fusion power plant, Fusion Eng. Des. **81** (2006) 469-476.

[11] N. Bekris et al., Assess Recovery Method of T from He Coolant; HCLL Processes and Components, TW2-TTBC-004 D2, Nuclear Fusion Programme Annual Report of the Association Forschungszentrum Karlsruhe/EURATOM Jan 2004-Dec. 2004, FZKA7117 EUR21526 EN.

[12] B. Bornschein, et al., Tritium management and safety issues in ITER and DEMO breeding blankets, Fusion Eng. Des. (2013), http://dx.doi.org/10.11016/j.fusengdes.2013.03.032.

[13] B. J. Merrill et al., Safety Assessment of the ARIES Compact Stellarator Design, Fusion Sci. Tech. 54 OCT.2008 838-863.

[14] Y. Song, Q. Huang, Y. Wang, M. Ni, Analysis on tritium controlling of the dual-cooled lithium lead blanket for fusion power reactor FDS-II, Fusion Eng. Des. **84** (2009) 1779-1783.

[15] L. El-Guebaly, S. Malang, Toward the ultimate goal of tritium self-sufficiency: Technical issues and requirements imposed on ARIES advanced power plants, Fusion Eng. Des. **84** (2009) 2072-2083.

[16] D.K. Sze, T. Q. Hua, M. A. Dagher, L. M. Waganer and M. A. Abdou, Tritium processing system for the ITER Li/V Blanket Test Module, Fusion Eng. Des. **39-40** (1998) 859-864.

[17] M.A. Abdou, E.L. Vold, C.Y. Gung, M.Z. Youssef and K. Shin, Deuterium-Tritium fuel self-sufficiency in fusion reactors, Fusion Tech. Vol. 9 MAR. 1986.

[18] W. Kuan and M.A. Abdou, A new approach for assessing the required tritium breeding ratio and startup inventory in future fusion reactors, Fusion Tech. Vol. 35 MAY 1999.

[19] M. Abdou, Grand Challenges with Exciting Opportunities for Young Researchers, Keynote Presentation at ISFNT-7, Tokyo, May 25, 2005.

[20] M.E. Sawan and M.A. Abdou, Physics and technology conditions for attaining tritium self-sufficiency for the DT fuel cycle, Fusion Eng. Des. 81 (2006) 1131-1144.

[21] G. Veredas, F. Fradera, I. Fernandez, L. Batet, I. Penalva, L. Mesquida, et al., Design and qualification of an on-line permeator for the recovery of tritium from lead-lithium eutectic breeding alloy, Fusion Eng. Des. **86** (2011) 2365-2369.

[22] P. Martinex, C. Moreno, I. Martinex and L. Sedano, Optimizing tritium extraction from a Permeator Against Vacuum (PAV) by dimensional design using different tritium transport modeling tools, Fusion Eng. des. **87** (2012) 1466-1470.

[23] L. A. Sedano, Tritium Cycle Design for He-cooled Blankets for DEMO, CIEMAT Internal Report 1110, June 2007.

[24] D. Demange, S. Staemmler and M. Kind, A new combination of membranes and membrane reactors for improved tritium management in breeder blanket of fusion machines, Fusion Eng. Des. 86 (2011) 2312-2316.

[25] V. Chuyanov et al., TBWG report for the period of the ITA, September 2005, Appendix 8-A Table 8-A-1.

[26] A.A. Harms, K.F. Scoepf, G.H. Miley, D.R. Kingdon, Principles of Fusion energy, World Scientific Publishing Co. Pte. Ltd., 2000, ISBN-13 978-981-033-3.

[27] F. Okino, K. Noborio, Y. Yamamoto, S. Konishi, Vacuum sieve tray for tritium extraction from liquid Pb-17Li, Fusion Eng. Des. 87 (2012) 1014-1018.

[28] M. Ichinose, Y. Yamamoto, K. Noborio, Y. Takeuchi, S. Konishi, "Preliminary Design of High Temperature Lithium-Lead Blanket with SiC Cooling Panel", ISBN 978-1-4244-2636-2/09 ©2009 IEEE, Proceedings of the 23rd symposium on Fusion engineering 2009.

[29] M.R. Spiegel, S. Lipschutz, and J. Lie, Mahtematical Handbook of Formulas and Tables 3rd ed. Schaum's Outlines, McGraw Hill Companies, ISBN 978-0-07-154855-7.

Ch. 5. Application of the instability theory for fusion reactor first wall

Summary of this chapter

This study proposes a probability of the evaporated gas that agitates a growing instability wave in a thin liquid film first wall. The liquid first wall was considered to be in vacuum and the effect of the ambient gas was neglected but the evaporated gas by the high energy fluxes is a probable cause of unstable wave agitation. The criterion is approximately expressed by the density ratio (Q_2) and the Weber number (We) as $Q_2 \times We^{0.5} \approx 5 \times 10^{-4}$. Performed indirect experimental supported this criterion. For a case study of liquid Pb-17Li film with a velocity of 10 m/s, the evaporated gas pressure must be below 6.2×10^3 Pa to maintain stable conditions. By recent study, this pressure is generated at 1600K temperature and it is believed to be attainable by the energy fluxes on the first wall. This result is so far not confirmed so the full verification by experimental is to be performed.

5.1 Introduction

Previous studies of the thin liquid metal film first wall for fusion engineering can be categorized into two groups. Here the liquid first wall includes the liquid film which flows along the internal wall and the straight free fall of the fusion core or ICF chamber. Both work as a first barrier from the high energy fluxes. The first group is primarily focused on the behavior and damage of the liquid film due to high-energy fluxes [1-8]. In these studies, fluctuations in the liquid film thickness are not considered. The second group of studies focuses on the fluctuation and stability of the liquid film, which is the approach taken in this study. Ying, Abdou [9] studied the criteria for fluid stability using the Reynolds number and the Weber number. Reperan, Yoda et al. [10, 11] observed flat flow stability and detachment, and Kondo, Suzuki et al. [12, 13] observed wave height distributions. Kunugi, Kawara et al. studied the design concept of stable free flow [14, 15]. Many other such studies have been conducted.

Thus far, the liquid metal film has been treated as in a vacuum condition, and the effect of an ambient gas was not considered as an instability factor. However, the authors predicted that the evaporated gas on the liquid metal film by high energy flux is a probable source of the ambient gas even in the vacuum chamber. To verify this effect, the critical condition of ambient gas for maintaining stable condition in a falling liquid film is analyzed. Then the effect of the evaporated gas is considered.

The liquid metal first wall is generally considered to flow along the large radius internal wall surface. But as far as the interaction between the liquid surface and the ambient gas, the free fall liquid film and the flow along the large radius wall do not behave differently, because both are in the surface tension domain. So the simple free fall model is assumed for the analysis and experimental.

5.2. Theoretical Analysis

5.2.1 Instability analysis

The growing wave formation was first analyzed by Squire [16] and Fraser [17] via the temporal single component method. The method was later expanded to a full complex analysis by Luca [18], Lin [19] and other forerunners. The instability wave on a liquid film is known to grow not only temporarily but also spatially. But as far as treating the large time asymptotic behavior and high We number condition, only the convective instability is known to remain, which is the disturbance propagates downstream with the group velocity U_g and grow temporarily and also spatially [20]. Due to the temporal non-dimensionalized factor $U_0/H_0 >> 1$ in this study, the convective instability is approximated as the temporal instability flows down with original flow velocity U_0. Hereafter, the normal temporal mode solution presented by Lin [20] is used for the analysis which is considered as an appropriate level method for this first step feasibility study.

5.2.2 Fluctuation wave equation

The small surface fluctuation of temporal instability is expressed as

$$f' = f_0 e^{i(kx-\omega t)} \tag{5.1},$$

where k, ω and f_0 are the non-dimensional wave number (real) of the x-axis, the complex angular frequency and an arbitrary constant (real), respectively. In this article, x-axis dimension is non-dimensionalized by H_0 as $x = x^*/H_0$, where x, x^* and H_0 is the x-axis dimensional length, non-dimensionalized length and half film thickness, respectively. At the free fall boundary condition, ω is known to have two independent, sinusoidal and varicose, wave mode solutions as expressed below [20].

$$\omega_s(k) = \omega_s^r \pm B_s^{1/2} = \frac{k\tanh(k)}{Q_2+\tanh(k)} \pm \sqrt{\left(\frac{1}{Q_2+\tanh(k)}\right)^2 \left\{\begin{array}{l}\frac{k^3}{We}\left(Q_2+\tanh(k)\right)\\ -k^2 Q_2 \tanh(k)\end{array}\right\}} \quad (5.2)$$

$$\omega_v(k) = \omega_v^r \pm B_v^{1/2} = \frac{k\coth(k)}{Q_2+\coth(k)} \pm \sqrt{\left(\frac{1}{Q_2+\coth(k)}\right)^2 \left\{\begin{array}{l}\frac{k^3}{We}\left(Q_2+\coth(k)\right)\\ -k^2 Q_2 \coth(k)\end{array}\right\}} \quad (5.3)$$

where superscript *r* means real number, subscript *s* and *v* means sinusoidal and varicose, respectively. Q_2 and *We* (Weber number) are defined as

$$Q_2 = \frac{\rho_2}{\rho_1}; \quad We = \frac{\rho_1 U_1^{\,2} H_0}{\sigma}$$

where ρ_2 and ρ_1 are the density of the ambient gas and the flowing liquid, respectively. U_1, H_0 and σ are the flow velocity, half of the liquid film thickness and the liquid surface tension, respectively. *Bv* and *Bs* are the discriminant of each equation. For a negative discriminant value, the wave grows exponentially.

5.2.3 Fastest growing wave number

Each discriminant of above equation (5.2) (5.3) is known to have a negative minimum. This minimum corresponds to the square of the fastest growing temporal amplitude. For Q2 << 1 and k < 1, the above discriminants can be simplified as

$$B_s(k) \approx \frac{k^2}{We} - kQ_2 \quad (5.4)$$

$$B_v(k) \approx \frac{k^4}{We} - k^3 Q_2 \quad (5.5).$$

By taking the derivative with respect to *k*, each independent fastest wave number can be described by equation(5.6), with a simple ratio of 2:3.

$$k_s^{\,m} : k_v^{\,m} = \frac{2Q_2 We}{4} : \frac{3Q_2 We}{4} = 2:3 \quad (5.6)$$

where superscript *m* means the fastest wave number.

As shown in Fig. 1, the two fastest growing waves merge and evolve to a single amplified wave. This situation is unfavorable for maintaining a stable liquid film thickness. The merged wave number k_{sp} can be described using each fastest wave number, as(5.8)

$$f_{sp}(x) = \sin\left(k_s^m x\right) + \sin\left(k_v^m x + \alpha\right) = 2\sin\left\{\frac{\left(k_s^m + k_v^m\right)}{2}x + \frac{\alpha}{2}\right\}\cos\left\{\frac{\left(k_s^m - k_v^m\right)}{2}x - \frac{\alpha}{2}\right\} \tag{5.7}$$

$$k_{sp} = \left|2\frac{\left(k_s^m - k_v^m\right)}{2}\right| = \left|k_s^m - k_v^m\right| \tag{5.8}$$

where, α is an arbitrary phase difference.

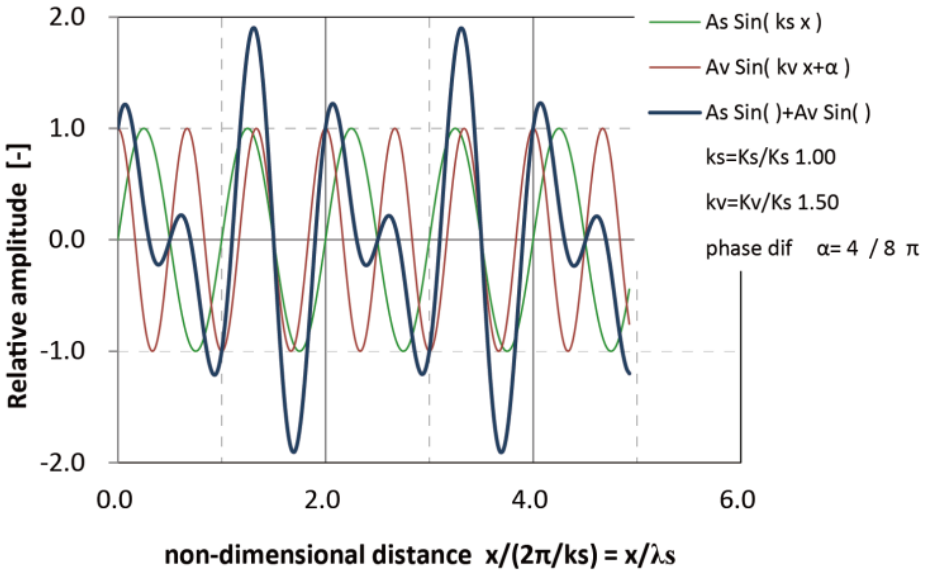

Fig. 1. Diagram of two superimposed waves.

Two independent waves (thin straight line) and a merged wave (bold line) are shown. The wave number ratio is 2:3, and the phase difference α is 1/2 π.

5.2.4 Critical condition of wave growth

The above two independent waves do not evolve unless each discriminant, *Bv* and *Bs*, has a negative minimum. Then, the density ratio Q_2 required to maintain both discriminants as positive is found from a numerical comparison of equations (5.2) and (5.3) for a given We number. The result is shown in Fig. 2. Beyond the triangles (upper right) is the wave growth zone. The critical condition is approximately expressed as

$$Q_2 \cdot We^{0.5} \approx 5 \times 10^{-4} \tag{5.9}$$

Below this line, the liquid film flow is stable, and the surface wave does not grow. For the case study of a Pb-17Li flow at a velocity of 10 m/s, the evaporated gas pressure must be below 6.2×10^3 Pa.

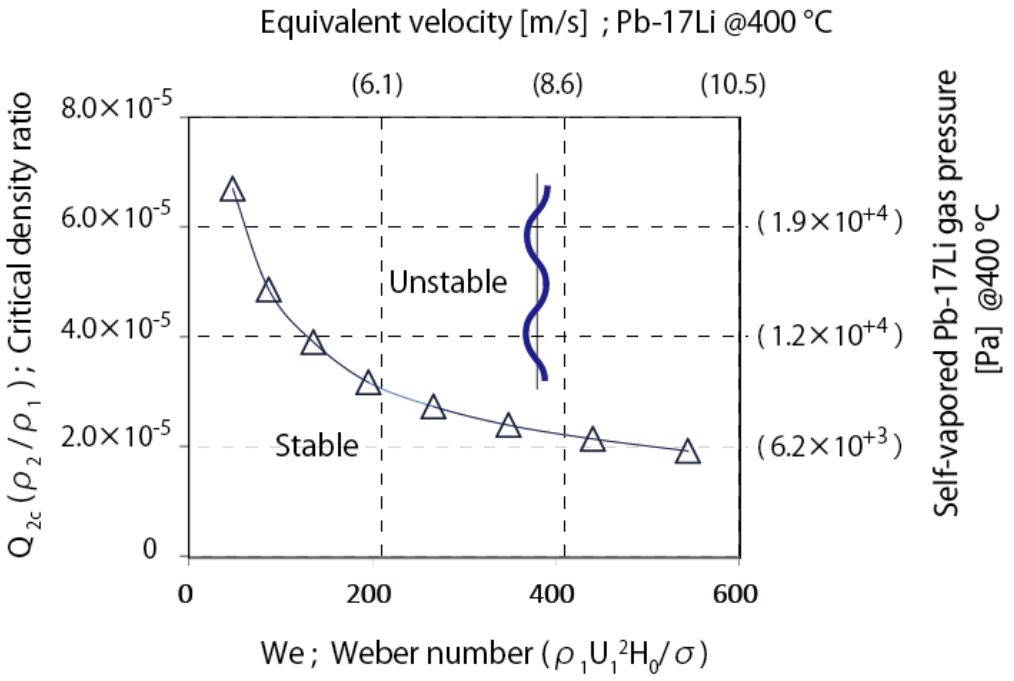

Fig. 2. Plots of the critical density ratio as a function of Weber number.

Below the triangles (lower left) lies the stable zone. This line is approximately expressed as $Q_2 \times We^{0.5} \approx 5 \times 10^{-4}$. As a reference, the velocity of liquid Pb-17Li and the evaporated gas pressure are given on a second scale.

5.3. Experimental

5.3.1 Verification method

To verify the deduced critical condition, described as Fig. 2, the experimental verification with the density ratio parameter and the We number parameter is mandatory. Though in this study, due to the limitation of experimental setup, the deduced fastest growing unstable wave number *ksp* Eq. (5.8) with the We number parameter was experimentally verified. The wave behavior of a liquid film is characterized by the non-dimensional Reynolds number, Froude number and Weber number. As shown in Table 1, liquid Pb-17Li and normal water exhibit similar wave motion behavior under this experimental condition. Thus, rather than liquid Pb-17Li, normal water was used for an experimental.

5.3.2 Experimental setup

An overall view of the experimental setup is shown in Fig. 3. Water liquid film was emitted from a 35-mm-wide slit with a 0.5-mm gap and then flowed down along two 350-mm-long knife-edge guides. Many previous studies about the thin liquid film first wall, the film thickness was assumed between 0.5 mm and 1 mm [9, 11, 22, 23]. To obtain enough gap and flow-width, gap and flow-length ratio, in this experimental, 0.5 mm was assumed. The initial velocity was calculated from the reading of the flow meter and the slit configuration. The initial flow velocity ranged from 4 m/s to 9 m/s. Below 3 m/s, breakup of the film occasionally occurred near the slit. For velocities higher than 9 m/s, breakup of the film also occurred.

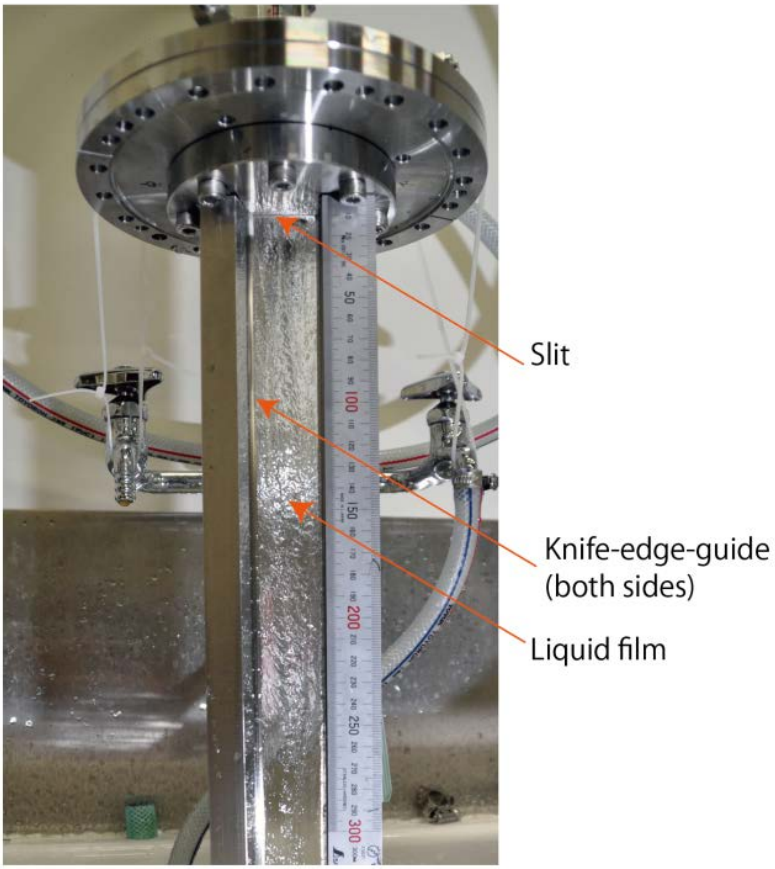

Fig. 3. Overall view of the experimental setup.

Liquid film is generated by a 35-mm-wide slit at the top with a 0.5-mm gap and then flows along the knife-edge between two guide-posts. The flow velocity ranged between 3 m/s and 9 m/s.

5.3.3 Observed wavelength

The surface fluctuation of the falling liquid film was observed by a digital camera as depicted in Fig. 4. To visualize the crest and the bottom of the wave as a difference in brightness, lighting was projected from lower 60 degree angle. In case of a wave-length of 1 mm, the critical detectable amplitude is 0.09 mm, which is appropriate level for this experimental. Difference of the amplitude, though it is not linear proportional, can be recognized as a difference of the shadow region which is described as a bold line length in Fig. 4.

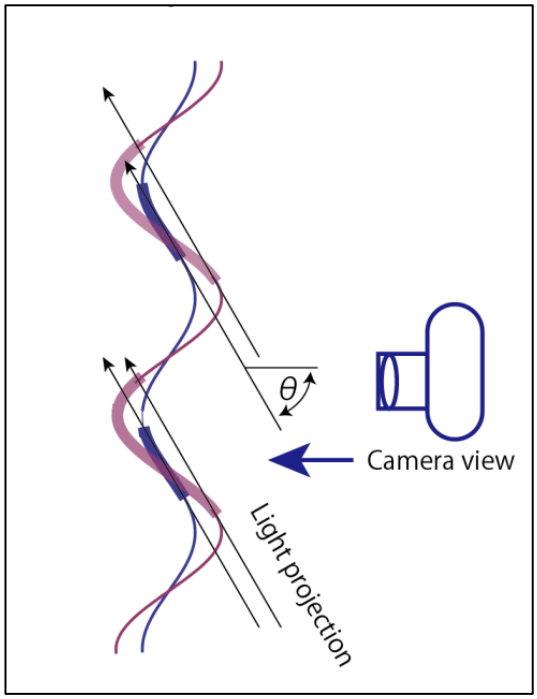

Fig. 4. A schematic of the light projection angle and the shadow region by the crest and bottom of wave front.

The shadow region is described by the bold line. The shadow region increases as the wave amplitude increases, though it is not proportional. By θ 60 degree projection, the wavelength 1mm with amplitude of 0.09 mm can be recognized.

The observed image example is shown in Fig. 5-a. The digitized result of the image is also shown in Fig. 5-b. The central flow region was analyzed, and both edge waves were eliminated. The surface density profile, which corresponds to the surface brightness, was normalized by 256 bits, as shown in Fig. 5-b.The largest amplitude wave component of the surface fluctuation was analyzed using the FFT method. The region of interest (ROI) was 180 mm long × 5 mm wide, and three different ROIs per surface were analyzed. The result for an 8-m/s flow surface is shown in Fig. 6.

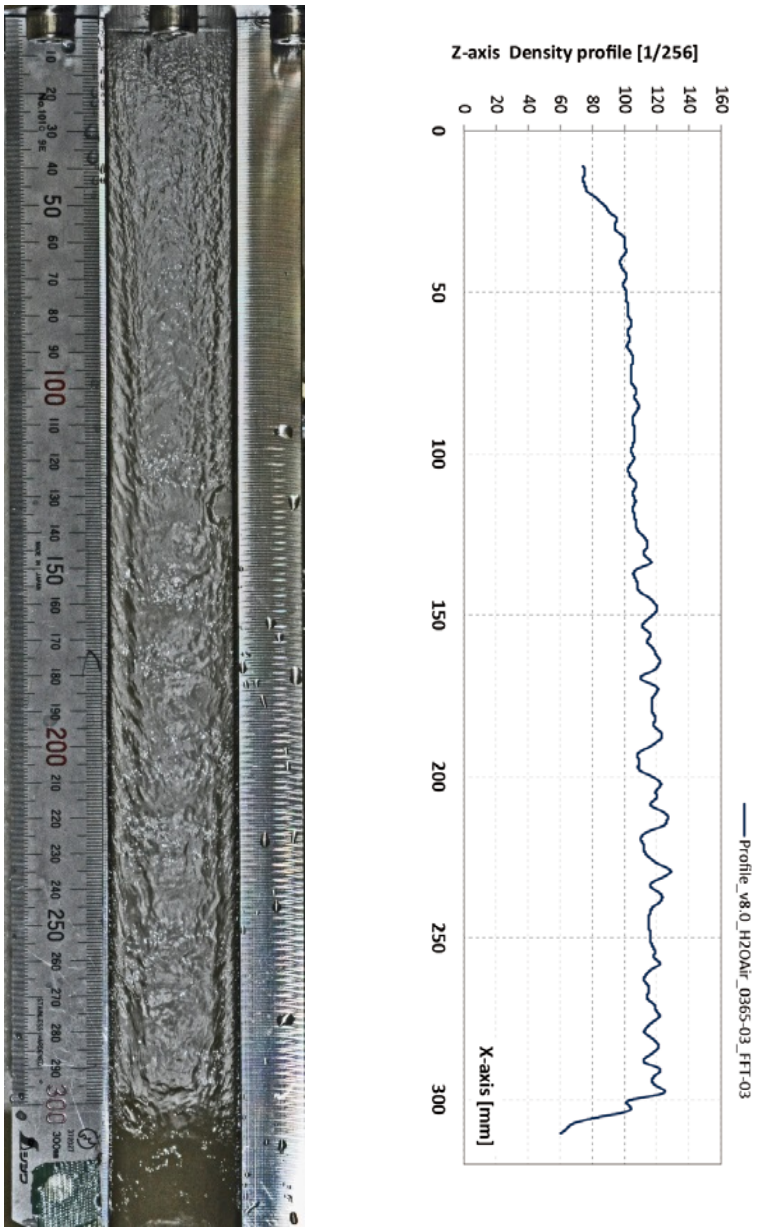

Fig. 5-a (Left). Photograph image of the observed water film surface fluctuation.

U_1 = 8 m/s, $Q_2 = 1.2\times10^{-3}$, We = $2.3\times10^{+2}$, $Q_2We^{0.5} = 1.8\times10^{-2}$. The vertical axis is the flow direction (x-axis). (Camera; Nikon D-7000 with Speed-light SB-600 lighting period 1/24000 sec.)

Fig. 5-b (Right). Density profile of the water film surface.

The left image was processed.

The horizontal axis is the 2^8 bit normalized density profile, corresponding to the darker and lighter regions of the right-hand image. Fluctuations of less than 1 mm were eliminated.

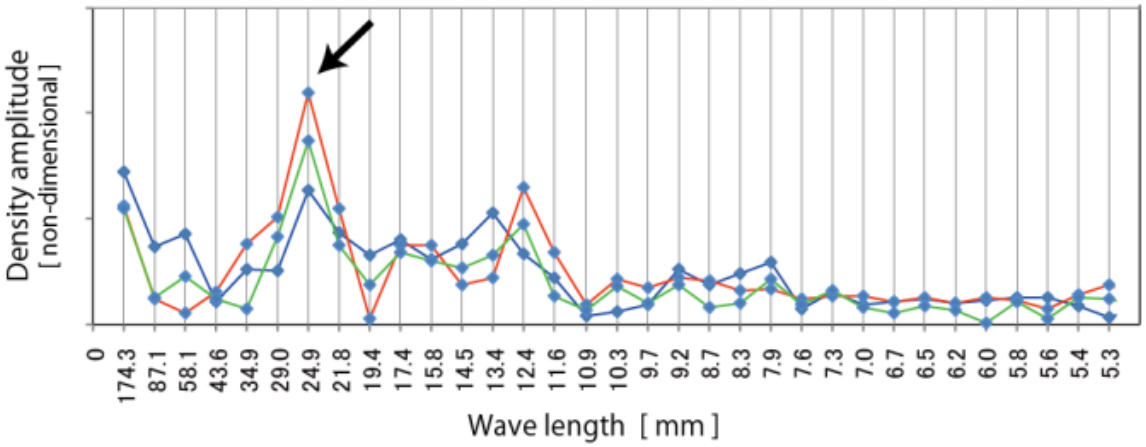

Fig. 6. FFT analysis results of the density profile of Fig. 5-b.

The horizontal axis is the wave-length of N-th Fourier series component. The vertical axis is the amplitude of each component of normalized density profile. Three results from different ROI on a Fig. 5-a are plotted in a same chart. The wave-length of 24.9 mm reveals the largest amplitude component of the surface fluctuation on a Fig. 5-a.

5.4. Results and Discussion

5.4.1 Results

The observed largest amplitude wave number and analytically predicted wave number are both plotted in Fig. 7. The predicted wave numbers showed good agreement with the observed results for We $\leq$ 230. At We = 290, the results deviated from the theory. A shift to another wave mode was predicted. These results confirm the initial stage of the wave growth process. Thus the unstable wave growth criterion on Fig. 2, which is deduced from the same instability theory, is indirectly supported.

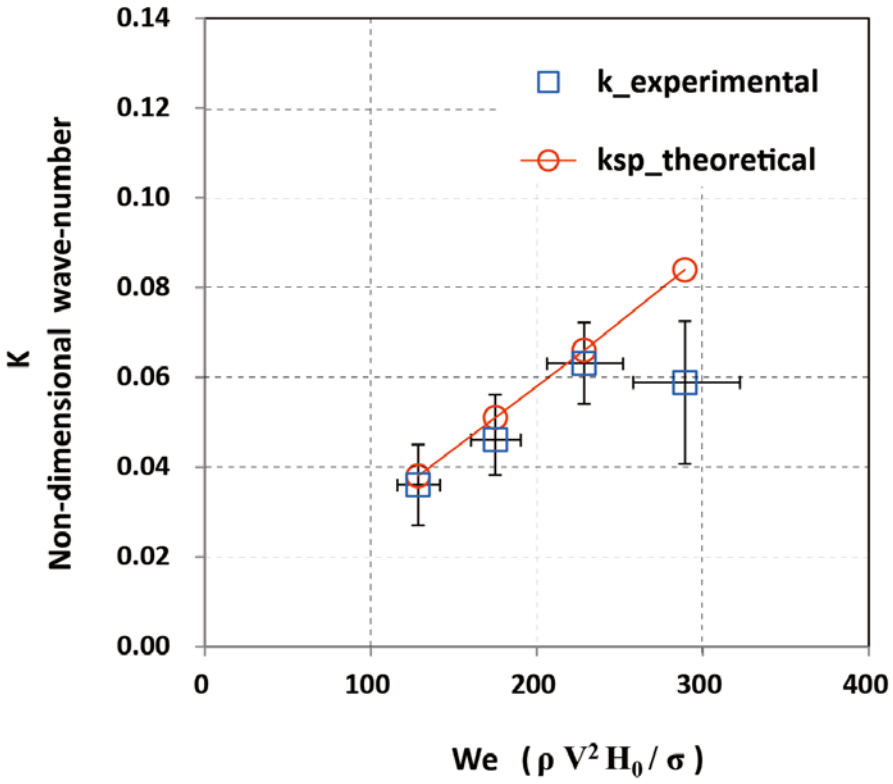

Fig. 7. The observed largest amplitude wave number k (□) as a function of Weber number (We).

The theoretically predicted largest amplitude wave number ksp (○) is also plotted.

At We < 230, the observed results agree with the theory. At We = 290, the observed results deviate from the theory. A shift to another wave mode is predicted to occur between 230 and 290, due to the decreasing growth time constant.

5.4.2 Discussions

5.4.2.1 Temporal and spatial instability

The attained results revealed the typical characteristics of the convective instability wave fluctuation. However, only by this digital picture result, it is not enough to determine. The observation of a wave propagation by the continuous motion pictures is mandatory. For further detail study, it should be considered.

5.4.2.2 Evaporated gas pressure

The predicted gas pressure at the critical condition of 10 m /s Pb-17Li liquid film flow, which is the typical velocity of the thin liquid metal film first wall concepts [9, 11, 22, 23], is approximately 6.2×10^3 Pa. According to the recent study about the evaporation of liquid Pb-17Li [21], this pressure is attained at approximately 1600 K temperature and it is presumed as a probable value by previous studies [1, 5, 6, 7, 24].

5.3. Conclusion

In this work, unstable wave growth of a thin liquid film first wall with ambient gas, particularly by an evaporated gas under vacuum condition, was examined.

By analytical study, the Weber number (We) and the density ratio (Q_2) of liquid and ambient gas are the primary factors of unstable wave growth. The deduced criteria is $Q_2 \cdot We^{0.5} \approx 5\times10^{-4}$ and performed experimental result is considered to support this.

For a case study of liquid Pb-17Li thin film of 10 m / s, the evaporated gas pressure at a critical condition is generated at 1600K temperature. It is predicted to be attainable under the high energy fluxes. This result might require some reconsideration for the feasibility of liquid first wall concept. But this criteria is not verified, so further examinations particularly by the full covered experimental are expected to be performed.

References

[1] M. A. Abdou and APEX Team, Exploring novel high power density concepts for attractive fusion systems, Fusion Eng. Des. 45 (1999) 145-167

[2] M. A. Abdou and APEX Team, On the exploration of innovative concepts for fusion chamber technology, Fusion Eng. des. 54 (2001) 181-247

[3] M. Uebeyli, Damage study for various materials at the first wall of a magnetic fusion reactor using protective liquid wall, Fusion Eng. Des. **83** (2008) 1508-511

[4] R.E. Nygre, T.D. Rognlien, M.E. Rensink, S.S. Smolentsev, M.Z. Youssef, M.E. Sawan et. al, A fusion reactor design with a liquid first wall and divertor, Fusion Eng. des. **72** (2004) 181-221

[5] N. B. Morley, Compressible response of thin liquid film/porous substrate first walls in IFE reactors, Fusion Eng. Des. **42** (1998) 563-568

[6] A. R. Raffray, D. Haynes and F. Najmabadi, IFE chamber walls: requirements, design options, and synergy with MFE plasma facing components, J. Nuc. Mat. **313-316** (2003) 23-31

[7] H. Furukawa, Y. Kozaki, K. Yamamoto, T. Johzaki and K. Mima, Simulation on interactions of X-ray and charged particles with first wall for IFE reactor, Fusion Eng. Des. **73** (2005) 95-103

[8] R. W. Moir, Liquid wall inertial fusion energy power plants, Fusion Eng. Des. **32-33** (1996) 93-104
[9] A. Ying and M. Abdou, Scaling Criteria for IFE liquid wall protection scheme simulation, Fusion Eng. Des. **42** (1998) 555-561
[10] J. J. R. Reperant, S. G. Durbin, M. Yoda, S. I. Abdel-Khalik and D. L. Sadowski, Studies of turbulent liquid sheets for protecting IFE reactor chamber first walls, Fusion Eng. Des. **63-64** (2002) 627-633
[11] M. Yoda, S. I. Abdel-Khalik and ARIES-IFE Team, An Investigation of the Fluid Dynamics Aspects of Thin Liquid Film Protection Schemes for Inertial Fusion Energy Reactor Chambers, Fusion Sci. Tech. **46** (2004) 451-469
[12] H. Kondo, T. Kanemura, H. Sugiura, N. Yamaoka, M. Ida, H. Nalamura et al., Development of measurement technique for surface waves on high-speed liquid lithium jet for IFMIF target, Fusion Eng. Des. **85** (2010) 1102-1105
[13] S. Y. Suzuki, H. Sugiura, E. Hoashi, H. Kondo, T. Kanemura, N. Yamaoka et al., Overview : Free surface measurement with renewed nozzle of Osaka Li loop, Fusion Eng. Des. **86** (2011) 2577-2580
[14] T. Kunugi , T. Nakai, Z. Kawara, T. Norimatsu and Y. Kozaki, Investigation of cascade-type falling liquid-film along first wall of laser-fusion reactor, Fusion Eng. Des. **83** (2008) 1888-1892
[15] Z. Kawara, K. Yamamoto, T. Kumugi and T. Norimatsu, Investigation of liquid-film formation along first wall of laser-fusion reactor, Fusion Eng. Des. **85** (2010) 2181-2186
[16] H. B. Squire, Investigation of the instability of a moving liquid film, Brit. J. Appl. Phys. **4** (1953), 167-169
[17] R. P. Fraser, P. Eisenklam, N. Dombrowski, and D. Hasson, Drop Formation from rapidly Moving Liquid Sheets, A. I. Ch. E. Journal Vol. **8** No. 5 (1962) 672-680.
[18] L.D. Luca and M. Costa, Instability of a spatially developing liquid sheet, J. Fluid Mech. **331** (1997) 127-144
[19] S. P. Lin, Z. W. Lian and B. J. Creighton, Absolute and convective instability of a liquid sheet, J. Fluid Mech. **220** (1990) 673-689
[20] S. P. Lin, Breakup of liquid sheets and Jets, Cambridge University Press 2003, ISBN 0-521-80694-1
[21] M. Kondo and Y. Nakajima, Boiling points of liquid breeders for fusion blankets, Fusion Eng. Des. 88 (2013) 2556-2559.
[22] R.W. Moir, HYLIFE-II Inertial Confinement Fusion Reactor Design, UCRL-JC-103816 Rev.1 (1991)
[23] H. Kondo, T. Furukawa, Y. Hirakawa, K. Nakamura, M. Ida, K. Watanabe et al., IFMIF/EVEDA lithium test loop: design and fabrication technology of target assembly as a key component, Nucl. Fusion 51 (2011) 123008 (12p)
[24] M.Z. Youssef, N. Morley, and A. El-Azab, X-Ray surface and volumetric heat deposition and tritium breeding issues in liquid-protected FW in high power density devices, 13th Topical Meeting on the Technology of Fusion Poer, June 7-11, 1998, Nashville, Tennessee.

Ch. 6. Closing

6.1 Wrap-up conclusion of the thesis

(1) Droplet diameter equation

The equation to describe the droplet diameter from a nozzle diameter is deduced, and confirmed by the experimental. It can be described only by a nozzle diameter and effected by no other properties.

(2) Mass transport enhancement from a droplet

The mass transport from a falling liquid PbLi droplet in vacuum showed two orders of magnitudes higher value than that of under static condition. The theoretically predicted contribution of deforming oscillation on the droplet is confirmed. This result drastically enlarged the design window for the liquid breeder extraction device.

(3) Tritium extraction device design

A case study of the tritium extraction device for the ITER class fusion reactor which uses liquid PbLi, is performed. The device diameter of 2.5 m, dropping height of 0.25 m with single stage design, showed enough capability to supply tritium under continuous burning condition. This configuration is well acceptable as a viable device design.

(4) Advantage of liquid droplet extractor

Based on above results, the tritium extraction method from a liquid PbLi in vacuum, i.e., the droplet extractor in vacuum, is proved as a viable device. The direct pumping in vacuum is the least energy consuming process than all other tritium extraction methods.

The comparison of the solid breeder tritium extraction, and liquid breeder are summarized as below.

	Solid breeder	Liquid breeder
advantage	● Extraction method pre-established ● Easy handling & maintenance (gas)	● **Simple & less energy consuming** ● Adjustable breeder composition ● No breeder damage
disadvantage	● High process energy consuming ● Breeder swelling & damage	● Handling difficulty (solidification) ● Erosion

(5) Instability theory application for the first wall of fusion reactor

The instability theory revealed as a strong tool for the analysis of liquid film PbLi . As an application, the critical condition of straight fall metal liquid-film is theoretically deduced. The

result suggest that the self-evaporating gas pressure of liquid film PbLi, which is aimed for the liquid first wall, might be the cause of the film instability, even though the inside of the fusion core is commonly regarded to be in vacuum.

6.2.1 List of Presentations

	名前	タイトル	会議名	会場	主催者	年月日	発表形態
1	興野 文人、登尾 一幸、山本 靖、小西 哲之	ﾘﾁｳﾑ鉛液滴中の落下中振動による溶解水素輸送	日本原子力学会2012 春の例会	福井大学	日本原子力学会	2012 年 3 月 19~21	口頭
2	興野 文人、登尾 一幸、笠田 竜太、小西 哲之	ﾄﾘﾁｳﾑ抽出装置における抽出能率とインベントリー推移に関する研究	第 9 回核融合エネルギー連合講演会	神戸ｺﾝﾍﾞﾝｼｮﾝｾﾝﾀｰ	日本原子力学会、ﾌﾟﾗｽﾞﾏ核融合学会	2012 年 6 月 28~29	poster
3	興野 文人、登尾 一幸、笠田 竜太、小西 哲之	リチウム鉛液滴の落下中振動による溶解水素輸送ーその2	日本原子力学会2012 秋の例会	広島大学	日本原子力学会	2012 年 9 月 19~21	口頭
4	F.Okino, K. Noborio, R. Kasada, S. Konishi	Tritium extraction from falling liquid Pb-17Li droplet	ANS 20th Topical Meeting on the Technology of Fusion Energy	Nashville, TN, USA	ANS	27~31-Aug-2012	poster
5	F.Okino, K. Noborio, R. Kasada, S. Konishi	Hydrogen transport mechanism in oscillating liquid Pb-17Li droplet	ANS 20th Topical Meeting on the Technology of Fusion Energy	Nashville, TN, USA	ANS	27~31-Aug-2012	poster
6	F.Okino, K. Noborio, R. Kasada, S. Konishi	Design and experimental verification of a tritium extraction process for liquid Pb-17Li by vacuum sieve tray	27th Symposium on Fusion Technology	Li'ege-Belgium	TEC	24~28-Sep-2012	poster
7	F.Okino, K. Noborio, R. Kasada, S. Konishi	Tritium extraction material behavior and hydoren tranport mechanism	2nd Japanese-German Workshop on Energy Materials Science	Karsruhe, Germany	KIT	11~14 December 2012	口頭
8	F.Okino, K. Noborio, R. Kasada, S. Konishi	Evaluation of the Stability of PbLi Liquid Film and its Possible Application	Japan-US Workshop on Fusion Power Plants and related Advanced technologies	Kyoto-Univ.	IAE	26-28 Feb 2013	口頭
9	興野 文人、登尾 一幸、笠田 竜太、小西 哲之	リチウム鉛液滴の落下中振動を利用したﾄﾘﾁｳﾑ抽出装置	日本原子力学会2013 春の例会	近畿大学	日本原子力学会	2013 年 3 月 26~28	口頭
9	興野 文人、笠田 竜太、小西 哲之	ﾘﾁｳﾑ鉛液膜の波動安定性と炉工学への適応検討	日本原子力学会2013 秋の例会	八戸工業大学	日本原子力学会	2013 年 9 月 03~05	口頭

10	F.Okino, R. Kasada, S. Konishi	Feasibility of a Liquid Film First Wall	11th International Symposium on Fusion Nuclear Technology	Barcelona, Spain	ISFNT	2013 Sept. 16-20	Poster
11	興野 文人、笠田 竜太、小西 哲之	ITER-TBM EU-HCLL を想定したトリチウム回収の検討	日本原子力学会 2014 春の例会	東京都市大学	日本原子力学会	2014 年 3 月 26~28	口頭

6.2.2 List of Publications

著者名	タイトル	ジャーナル名	Vol.	No.	page（始）	page（終）	発行年	
F. Okino, K. Noborio, Y. Yamamoto, S. Konishi	Vacuum sieve tray for tritium extraction from liquid Pb-17Li	Fusion Engineering and Design	Volume 87		1014	1018	2012	
F. Okino, K. Noborio, R. Kasada, S. Konishi	Enhanced mass transfer of deuterium extracted from falling liquid Pb-17Li droplets	Fusion Science and Technology	Volume 64	3	543	548	2013	
F. Okino, K. Noborio, R. Kasada, S. Konishi	Deuterium transport prediction in oscillating liquid Pb-17Li droplet	Fusion Science and Technology	Volume 64	3	549	551	2013	
F. Okino, R. Kasada, S. Konishi	Study on flow instability for feasibility of a thin liquid film first wall	Fusion Engineering and Design	Volume 89		1054	1058	2014	
F. Okino, K. Noborio, R. Kasada, S. Konishi	Design and study of a tritium extraction device with a vacuum sieve tray and liquid Pb-17Li blanket	Fusion Engineering and Design	FUSENGDES-D-13-00080				2013	submitted

6.3 Acknowledgements

Many portion of this work is supported by the Global COE program of Kyoto University " Toward CO_2 Zero-emission System" and I express my sincere thanks to the organization.

This work is not completed without the suggestive advices based on their genius intuitions and insights on all over the thesis by Prof. Konishi, and Prof. Kasada. Also this work is not completed without the well experienced advices on experimental by Prof. Yamamoto and Dr. Noborio. As to the theories required for this work, i.e., the continuum theory, vector analysis, hydro-dynamics and instability theory, the advices by Prof. Hoshide and Prof. Imatani were inevitable for analytical considerations. Here I sincerely express my appreciation to their devotions.

While performing this wok, I encountered many unknown, unexperienced physical phenomena. To comprehend these subjects, I studied mass transport theory under advection, convective instability theory of liquids, and many other subjects. Particularly following literatures are so called "books always with me" and I repeatedly re-read them. So it is unusual but here I sincerely appreciate the elaborating woks by the authors, and express my sincere thanks by listing the title of them.

R.Byron Bird, Warren E. Stewart and Edwin N. Lightfoot, " Transport Phenomena 2nd ed.", John Wiley & Sons, Inc.

E.L. Cussler, "Diffusion; Mass Transfer in Fluid Systems 3rd ed., Cambridge University Press.

J. Crank, "The Mathematics of Diffusion 2nd ed.", Oxford University Press.

S.P. Lin, "Breakup of Liquid Sheets and Jets", Cambridge University Press.

S. Chandrasekhar, "Hydrodynamic and Hydromagnetic Stability", Dover Publications, Inc.

F. Charru, "Hydrodynamic Instabilities", Cambridge University Press.

P-G de Gennes, F. B-Wyart and D. Quere, "Capillarity and Wetting Phenomena", Springer.

And many other books not listed here.

---- End of the thesis ----